ELASTIC-PLASTIC RESPONSE OF BEAMS INCLUDING EFFECTS OF SHEAR AND ROTATORY INERTIA

Thesis for the Degree of Ph. D.

MICHIGAN STATE UNIVERSITY

B. Nurel Beyleryan

1965

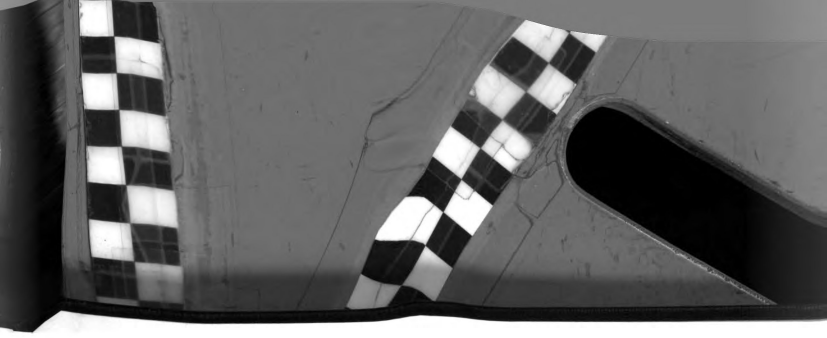

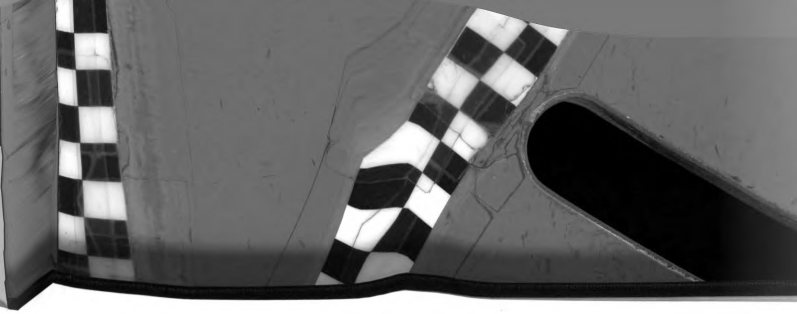

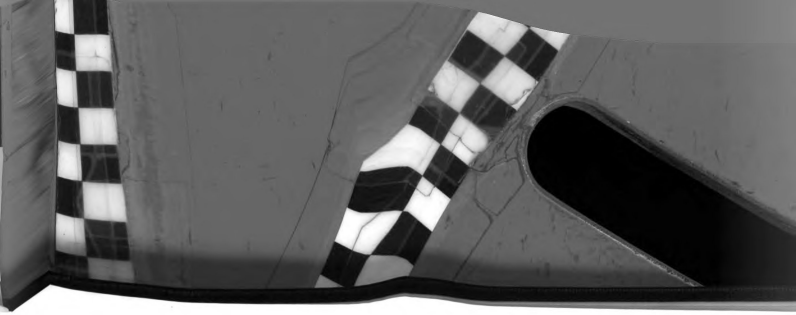

ABSTRACT

ELASTIC-PLASTIC RESPONSE OF BEAMS
INCLUDING EFFECTS OF SHEAR AND ROTATORY INERTIA

by B. Nurel Beyleryan

In this investigation a physical model is constructed in which the shear deformation and rotatory inertia of a continuous beam, in addition to the bending deformation and lateral displacement inertia, are lumped at a discrete number of points. The model thus consists of rigid panels connected by shear and moment springs. The interaction between moment and shear on the material behavior at yield is taken into account. The mass, rotatory inertia, and external loading of the panels are lumped at the center of each panel.

Solutions are obtained by numerical techniques, which have been programmed in the Fortran language for use on the CDC3600 system of Michigan State University. The convergence of the discrete model is indicated by the increasing degree of agreement of the numerical results as the beam is divided into larger numbers of panels.

Numerical results are then obtained for simply supported and fixed-fixed beams subjected to a blast type loading. Taking the web thickness and the beam length of an I-beam as parameters, the

influence of the interaction between moment and shear is studied. It is shown that, as expected, as the web thickness or the span length is increased, the elastic-plastic solution including shear and rotatory inertia effects (the "Timoshenko" model) approaches that of the simple theory (the "Euler" model).

For steel I-beams of usual proportions, the influence of shear and its interaction with moment was found to be quite significant for fixed-fixed beams and to a lesser extent for simply supported beams.

The discrete model is also reduced, for the elastic case, to lesser forms such as one that excludes the effect of rotatory inertia. However, it is found that, rather unexpectedly, the computer time required when using the complete model is no more than any of the reduced models. The latter, therefore, do not seem to offer any practical advantage.

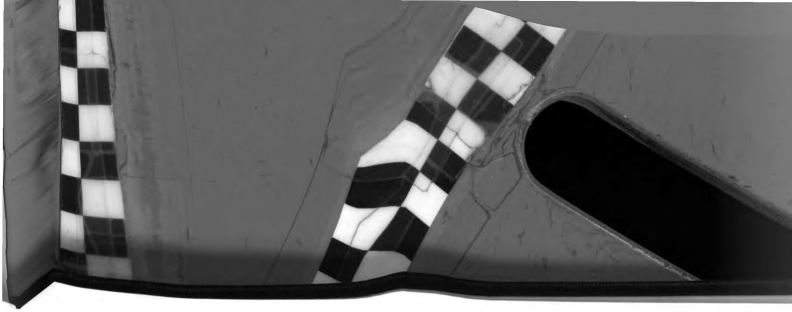

ELASTIC-PLASTIC RESPONSE OF BEAMS INCLUDING EFFECTS OF SHEAR AND ROTATORY INERTIA

by

B. Nurel Beyleryan

A THESIS

Submitted to
Michigan State University
in partial fulfillment of the requirements
for the degree of

DOCTOR OF PHILOSOPHY

Department of Civil and Sanitary Engineering

1965

ACKNOWLEDGMENTS

The author wishes to acknowledge the valuable guidance of Dr. R. K. Wen, under whose direction this study was conducted. Thanks are also extended to the members of the author's Guidance Committee, Dr. C. E. Cutts, Dr. L. E. Malvern, Dr. G. E. Mase, and Dr. C. P. Wells, for their interests and help during the course of the author's studies at Michigan State University.

The author wishes to express his special appreciation to the Chairman of the Civil Engineering Department, and the Head of the Engineering Research Division, for their support of the author's doctoral program.

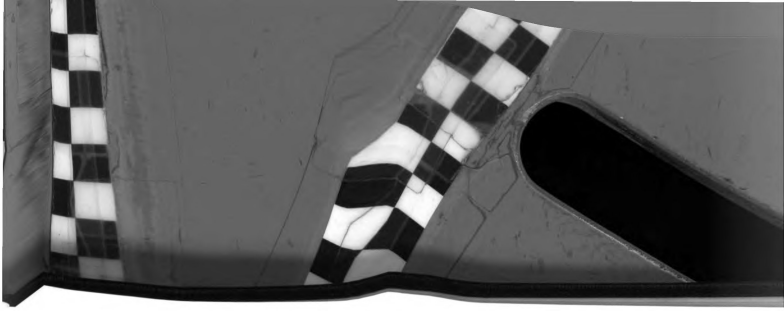

TABLE OF CONTENTS

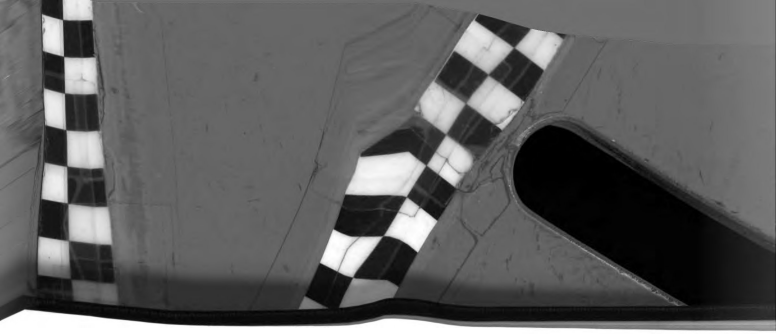

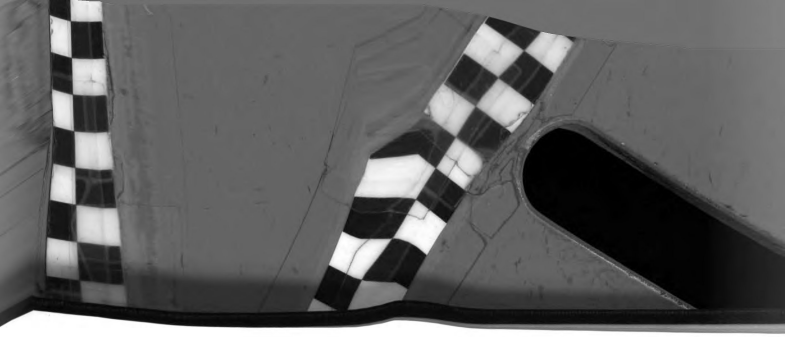

LIST OF FIGURES

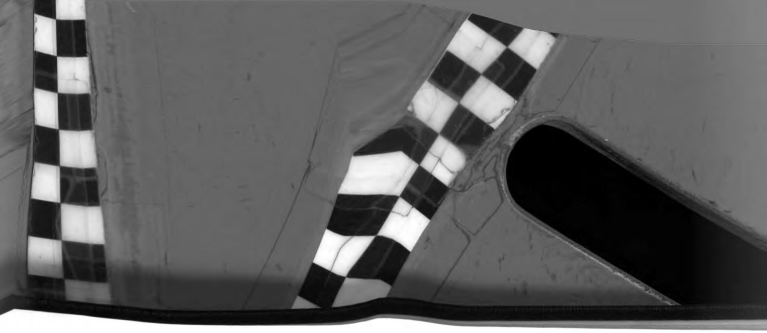

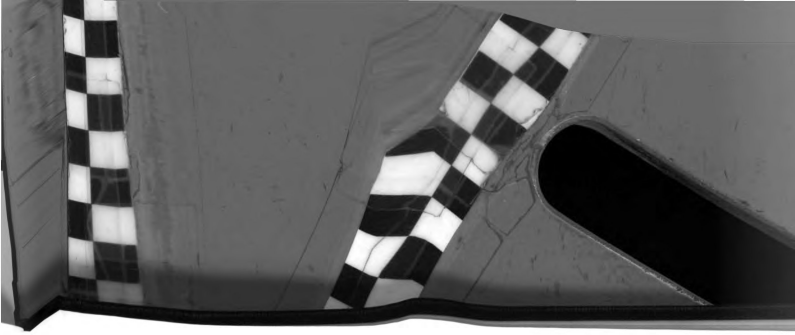

I. INTRODUCTION

1.1. General

It is well known that the usual engineering theory of beam vibrations is based on the assumptions that deformations are caused by bending only, and only transverse inertia forces need be considered. In particular, the theory neglects the effects of shear deformations and rotatory inertia.

The first modification of the theory by including the above mentioned effects was given as early as 1859, by Bresse (8); but, apparently it went unnoticed. Rotatory inertia effects were also discussed by Raleigh (36) in 1877. Today, for the more exact theory that includes shear deformation and rotatory inertia effects, the presentation of Timoshenko (41) is usually quoted. In fact, it is known as the "Timoshenko" beam theory. A derivation of this will be given in Section 2.1.

For several decades, after Timoshenko's contribution, work was generally directed towards obtaining estimations of the error introduced if effects of shear deformation and rotatory inertia were neglected. Solutions obtained with substantial rigor for various special cases of the problem have appeared since 1948. Two approaches seem to dominate the literature covering the elastic

vibrations of the Timoshenko beam: the wave method (7, 12, 21, 27), and the mode method (1, 4, 10, 20, 40, 43). The former usually employs Laplace transform techniques to yield solutions in closed form. The complicated superposition required, in order to accommodate various loading and boundary conditions, makes the method rather unwieldy to apply. The mode method, presented in full in Reference1, has also proven to be inconvenient for applications to actual problems. Furthermore, convergence of the solution is not always guaranteed.

While the preceding discussion applies to the linearly elastic case, the literature on the inelastic case is rather scarce. Two articles, by Salvadori and Weidlinger (38), and Karunes and Onat (22) dated 1957 and 1960, respectively, have considered the rigid-plastic response of beams. It is found in the former work that, in case of a simply supported beam, "plastic shear hinges" may develop at the supports in addition to a moment hinge at the mid-span of the beam. In the latter study, a free-free, rigid-plastic beam subjected to a concentrated load at the mid-span is investigated. In both references, the methods used can not deal with the interaction effects between the bending moment and shear when the material goes into the plastic range. Yet, this interaction is known to exist, and its effects on beam vibrations have not been ascertained.

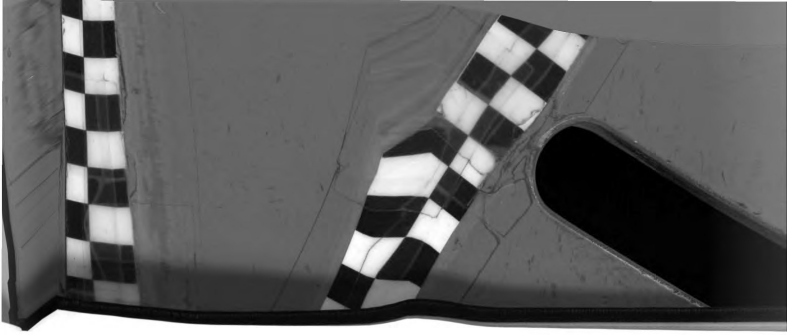

The previous paragraphs point out clearly what has been missing so far; namely: a method of analysis which can be used to calculate the elastic-plastic vibrations of beams, including shear deformation and rotatory inertia effects, with any usual boundary conditions, and subjected to any usual loading. This will be the general purpose of the present investigation.

Thus, the first objective of the present work is to develop such a method. The second objective is to use the method to study the significance of the effects of shear deformation and rotatory inertia on the beam response in the inelastic range.

Recognizing the intrinsic difficulties of the problem, particularly from a continuum point of view, the present work uses the discrete model approach. Briefly, the model used to represent the beam consists of rigid panels connected by moment and shear springs. The force-deformation characteristics of these springs interact when the deformations are in a plastic state. At the middle of the panels, there are lumped masses on which the external loads act. This model is amenable to analysis and numerical results are conveniently obtainable from a computer.

Of course, it is not sufficient that the model produces results. It is also necessary to show that such results are trustworthy. To this end, the obvious way is to compare the model results with the

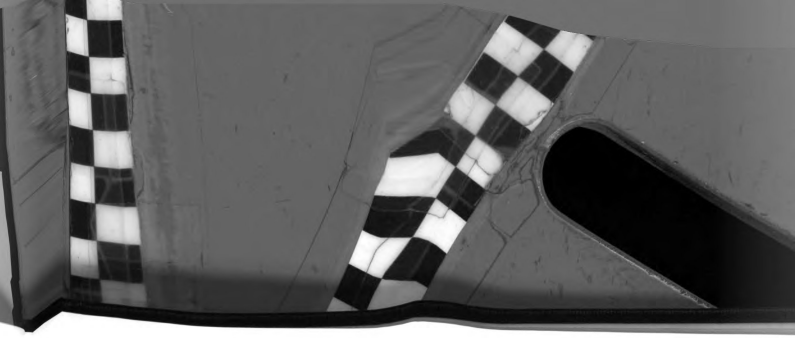

exact analytical solutions (of the continuum). But exact solutions are not readily available. Hence, the credibility of the model is examined by comparing the numerical results yielded by models with different degrees of fineness (analogous to the mesh size in a formal finite difference approach). If the results seem to converge (referred to later as "apparent" convergence), then the model is regarded as reliable.

There is an exception to the above approach. For one of the "reduced forms" of the model, exact solutions are available--and used for comparison. Furthermore, the reliability of the model is also judged from a physical point of view in that the behavior, as exhibited by the model results, must make good physical sense.

In pursuit of the second major objective of this thesis, the model is used to obtain numerical results that would reflect the significance of shear deformation and rotatory inertia in elastic-plastic response. The data cover both simply supported, and fixed-fixed beams. In order to highlight the shear effects, I-beams alone are considered. The variables considered are the total permanent deflection, the permanent deflection due to shear effects alone, as well as the maximum deflection. Parameters considered are the web thickness and span length. The web

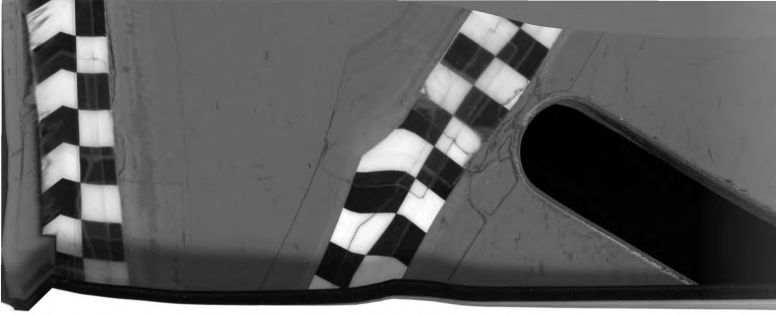

thickness will be varied from 20% to 3% of the flange width and the length will be varied from 6 to 20 times the beam depth.

In the remaining chapters of this thesis, the theoretical bases of this work are presented in Chapter II, and the numerical technique is presented in Chapter III. Chapter IV and Chapter V contain, respectively, the elastic and elastic-plastic numerical results. Concluding remarks are made in Chapter VI.

1.2. Notations

The notation listed below has been adopted in this investigation.

α = Lumped change of curvature;

α_e = Elastic part of α ;

α_p = Plastic part of α ;

α_y = Elastic change of curvature, corresponding to a change of moment $\Delta M=M_y$;

$\overline{\alpha}$ = α/α_y

β = Shear displacement (slide);

β_e = Elastic part of β ;

β_p = Plastic part of β ;

β_y = Elastic change of shear slide, corresponding to a change of shear $\Delta S=S_y$;

$\overline{\beta}$ = β/β_y

β' = β divided by its tributary length;

Δ = Prefix denoting "increment";

ρ = Density of material;

τ = Time in plastic range;

ϕ = Slope of a panel of the model;

$\dot{\phi}$ = Change of ϕ with respect to time;

$\ddot{\phi}$ = Rate of change of $\dot{\phi}$ with respect to time;

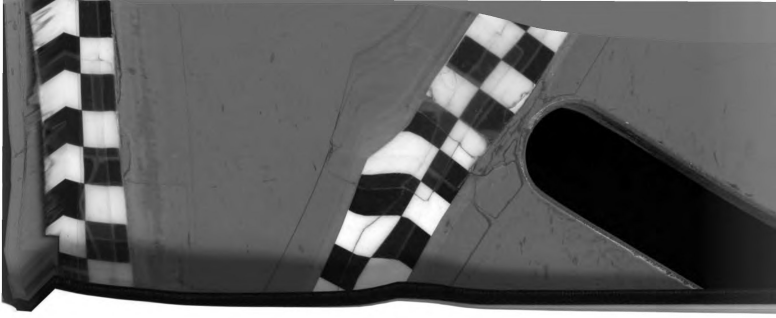

A = Cross-sectional area of the beam;

B = Half of the flange width;

b = A boundary constant;

c = Arbitrary coefficient pertaining to applied load;

d = Vector with components $\Delta\bar{\alpha}$ and $\Delta\bar{\beta}$;

E = Elastic modulus of the material;

$f(M, S)$ = Plastic potential function;

G = Shear modulus of the material;

g = Gravitational constant;

H = Half of the beam depth;

h = (Subscripted or not) Length of a panel;

I = Moment of Inertia;

i = Variable subscript to denote a point or a segment on the beam;

j = The highest value of i;

K_i = Constants;

k' = A cross-sectional constant;

L = Length of beam;

M = Moment;

M_y = Maximum moment at yield;

m = Non-dimensional moment M/M_y;

m_i = Lumped mass;

N, n = Number of panels into which a beam is divided;

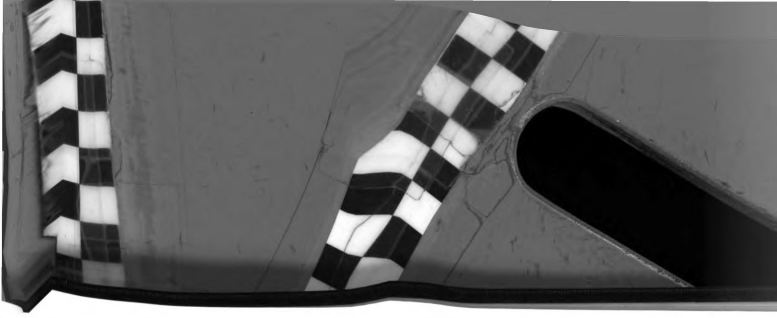

P_i = Lumped external loads acting on panel i;

S = Shear;

S_y = Maximum shear at yield;

s = Non-dimensional shear S/S_y;

T = Flange thickness of I-beam;

T_1 = Period of the fundamental mode of vibration;

T_n = Period of the n-th mode of vibration;

t = Time;

t_o = Initial time;

t_w = Web thickness;

$\bar{t}$ = Non-dimensional time t/T_1;

$\bar{t}_w$ = Non-dimensional web thickness $t_w/(2B)$;

W = Minimum stationary loading that will cause yield for a simply supported beam;

w(x, t) = Loading as a function of position and time;

x = Length coordinate;

Y_y = Static deflection caused by a uniformaly distributed load of W;

y = Vertical direction (unsubscripted);

y = Deflection of the beam (subscripted);

$\dot{y}$ = Velocity;

$\ddot{y}$ = Acceleration;

y' = Slope;

$\bar{y}$ = Non-dimensional deflection y/Y_y.

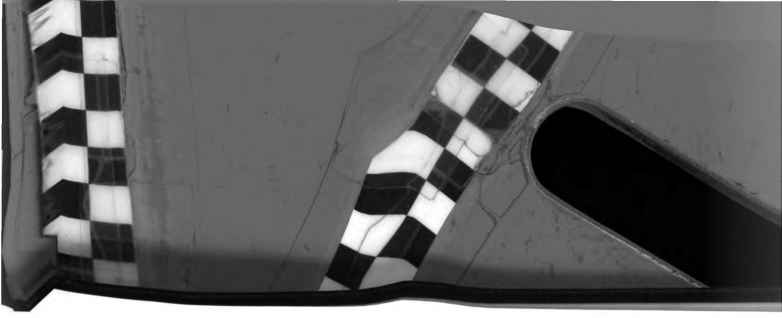

II. BASES OF ANALYSIS

2.1. Continuum Theory

For the sake of completeness, a derivation of the more exact beam equations including the effects of shear deformation and rotatory inertia will be given below for a physical continuum (41).

When a beam deforms, its slope $\frac{dy}{dx}$ (or y') may be considered to consist of two parts: ϕ, the slope due to bending only, and $\frac{d\beta}{dx}$ (or β'), an additional slope due to shear (β denotes the shear deformation or "slide"). Therefore,

$$y' = \phi + \beta' \qquad 2.1$$

The kinetic equations can be obtained from D'Alembert's principle by summing the vertical forces and the moments. Referring to Figure 2.1, one can write:

$$\frac{\partial S}{\partial x} = \rho A \frac{\partial^2 y}{\partial t^2} - w(x, t) \qquad 2.2$$

$$S = \frac{\partial M}{\partial x} + \rho I \frac{\partial^2 \phi}{\partial t^2} \qquad 2.3$$

where t is time, A is the cross-sectional area, ρ is the density, and I is the moment of inertia; the other symbols are defined in the figure.

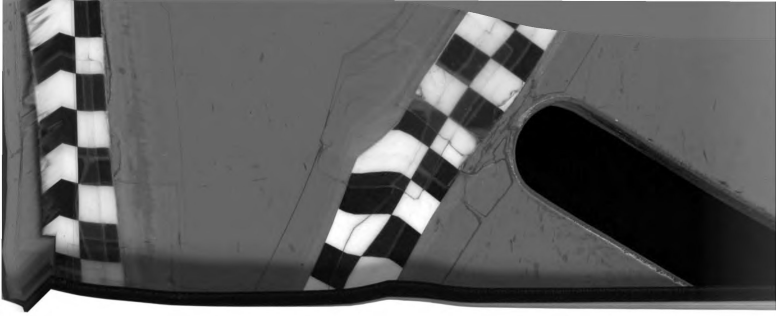

Equation 2.1 is obtained from a consideration of geometry, and Equations 2.2 and 2.3 from equilibrium. Thus, they are general and valid for all materials. Further relations needed for an analysis must be obtained from the properties of the material.

For an elastic and isotropic material one can write,

$$M = - EI \frac{\partial \phi}{\partial x} \qquad 2.4$$

$$S = Gk'A\beta' \qquad 2.5$$

where E is the elastic modulus, G is the shear modulus, and k' is a sectional constant. For elastic beams, Equations 2.1 through 2.5 can be combined into a smaller number of equations, as various investigators have done (if combined into one fourth order partial differential equation, it becomes the "Timoshenko" beam equation (41)). However, since plastic as well as elastic cases will be treated herein, the equations will not be combined at this point.

Equations 2.4 and 2.5 must be replaced by suitable relationships when the deformations go beyond the elastic range. When this happens, the material is assumed to be perfectly plastic. The term "perfectly plastic" is used here to mean that no work-hardening effects are considered. (As long as the material is not strained excessively, most mild steel can be assumed to be perfectly plastic.)

The inelastic behavior will be assumed to be governed by the "plastic potential theory" (19), which is briefly explained below for

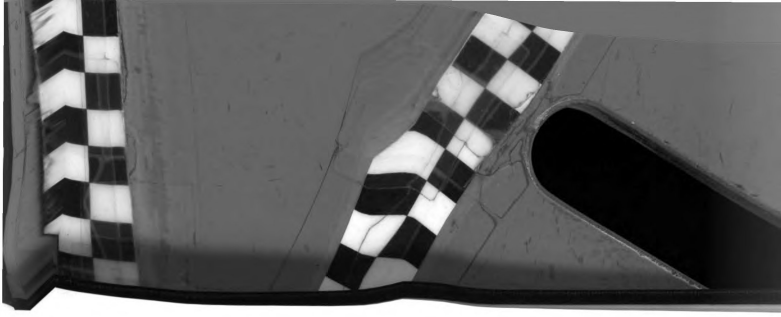

the problem under consideration.

Associated with a given cross-section there is a plastic potential function f(M, S). The curve in the M-S plane:

$$f(M, S) = 0 \qquad 2.6$$

is known as the "yield curve" or the "interaction curve." This is illustrated in Figure 2.2 for the positive quadrant.

When the values of M and S acting at the section are such that $f(M, S) < 0$, the laws of elasticity apply. When $f(M, S) = 0$, the section is in a plastic state, and yielding or plastic deformation takes place. The value of f(M, S) can never be positive.

When plastic deformation occurs, it is governed by the following rule: the rate of the plastic deformation corresponding to M (or S) is proportional to the M-component (or S-component) of the gradient ∇f, or the normal to the interaction curve; see Figure 2.2. Expressed mathematically, yielding is to follow the relation:

$$\frac{\frac{\partial f(M, S)}{\partial M}}{\frac{\partial}{\partial t}\left(\frac{\partial \phi}{\partial x}\right)_p} = \frac{\frac{\partial f(M, S)}{\partial S}}{\frac{\partial}{\partial t}\left(\frac{\partial \beta}{\partial x}\right)_p} = K_1 \qquad 2.7$$

in which the subscript p denotes the plastic component of the deformations, and K_1 is a scalar.

A simultaneous solution of the preceding equations, even for the elastic case, has proven to be very difficult. For the

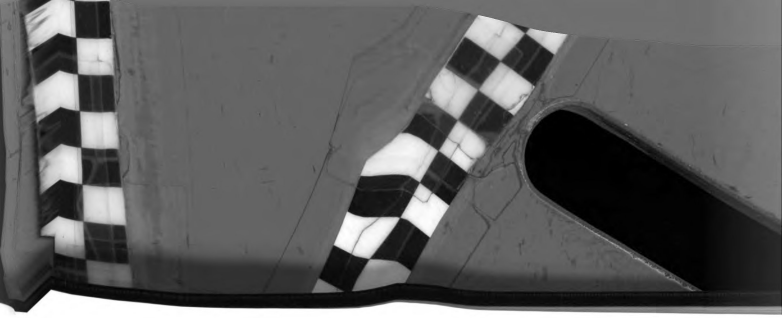

elastic-plastic case, an analytical solution seems almost impossible. One could try the usual finite difference approach. However, he would soon encounter difficulties in the treatment of boundary conditions and the changing material properties.

2.2. Discrete Theory

In order to obtain an approximate solution of the problem, the present author suggests the use of a discrete model for the beam. It is understood that changing a continuous beam into a discrete model inevitably involves a loss in "resolution" and even some distortion. However, it is believed that the essential features of the beam have been kept in the model.

Figure 2.3 illustrates the discrete beam in an undeformed state, and Figure 2.4 shows the deformed configuration of the model. The various properties of continuum are retained in a manner as given below.

a) The continuous beam is divided into a discrete number of panels, N. These panels may, in general, be of different lengths, h_i.

b) The panels are assumed rigid at all times. However, in order to account for the deformations and rotations that a continuous beam undergoes, moment and shear springs are inserted between the rigid panels. The sections where these springs are

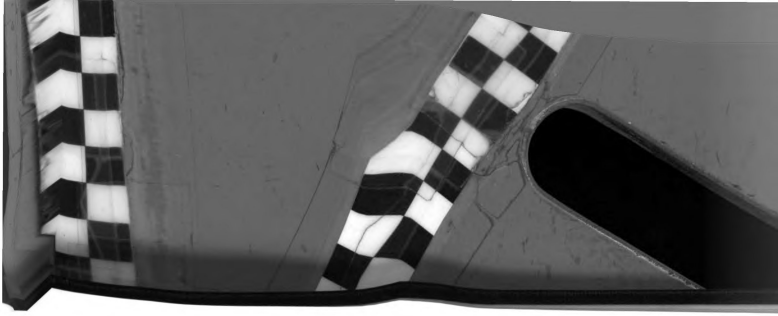

placed are called the "force points."

c) The rotation of a moment spring corresponds to the sum of the curvature within a length of h/2 on either side of the panel point; that is, the flexibility of a panel is lumped equally at the springs to the left and right of a panel. At a typical spring i, the lumped elastic flexibility is $2EI/(h_{i-1}+h_i)$.

d) Similarly, a shear spring lumps the shear flexibility from a tributary length of h/2 on either side of the panel point. For example, the flexibility of the i-th shear spring is $2Gk'A\,\beta_i/(h_{i-1}+h_i)$.

e) In inelastic action, when interaction is considered between shear and moment, the moment and shear springs are made to obey laws that are direct generalizations of the plastic potential theory described earlier for a cross-section of the continuous beam. Detailed description of the procedure is given in Section 3.2.

f) The mass and rotatory inertia within each panel are lumped at the center of the panel, which is referred to as a "mass point." The external loading will be similarly lumped. In Figure 2.4 the symbols m_i, $(\rho Ih)_i$, P_i, denote, respectively, the lumped mass, rotatory inertia, and load.

Some of the implications of this model may be noted here as follows. The characteristic of rigid panels gives the beam a

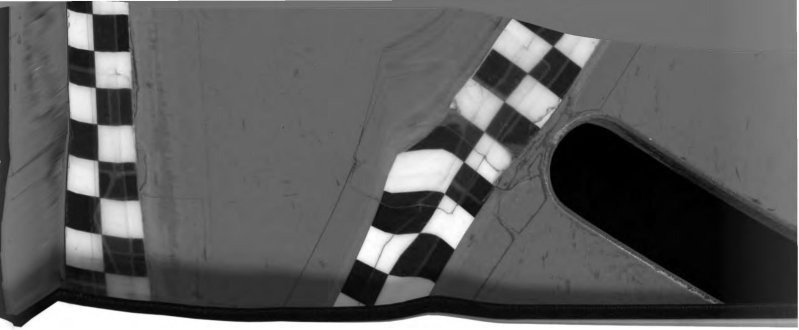

discontinuous look. In particular, the deflections are discontinuous at the shear springs. Consequently, the apparent slope of a segment is given by ϕ_i , which is the slope due to flexure alone.

Since equations of motion will be written for the mass points, deflections are defined only at mass points; stress resultants are defined only at the force points. It is also apparent that concentrated external loads must be applied at mass points. As a consequence of the lumping, one might expect that the displacements, moments, and shears essentially represent the values of the corresponding quantities in the continuum, averaged over appropriate lengths.

Relations regarding boundary conditions between the model and continuum will be dealt with in Section 2.4.

The equations governing the motion of a discrete beam system are written in the same way as for a continuous beam. However, the infinitesimal increment along the beam is replaced by a segment of finite length, h_i.

Writing the equation of motion in the vertical direction for a typical panel i, (Figure 2.5) one obtains,

$$m_i \frac{\partial^2 y_i}{\partial t^2} = S_{i+1} - S_i + P_i \qquad 2.8$$

Similarly, the equation for rotatory motion becomes

$$(\rho Ih)_i \frac{\partial^2 \phi_i}{\partial t^2} = M_i - M_{i+1} + \frac{h_i}{2} (S_i + S_{i+1}) \qquad 2.9$$

If elasticity prevails, the constitutive equations are, in discrete form

$$M_i = \frac{-2EI\alpha_i}{h_i + h_{i-1}} \qquad 2.10$$

and

$$S_i = Gk'A\beta_i \frac{2}{h_i + h_{i-1}} \qquad 2.11$$

where α_i and β_i denote, respectively, the deformations of the moment and shear springs. They are related to y_i and ϕ_i by geometry and the relations are given in Section 3.2.

When plastic yielding is considered, Equations 2.6 and 2.7 are applied to the springs of the discrete beam. At a force point, the yield curve is given by

$$f(M_i, S_i) = 0 \qquad 2.12$$

This is similar to Equation 2.6 which pertains to a cross-section of the continuum. Since the curvature and the shear slide are lumped at the force points, Equation 2.7 can be generalized for a typical force point as

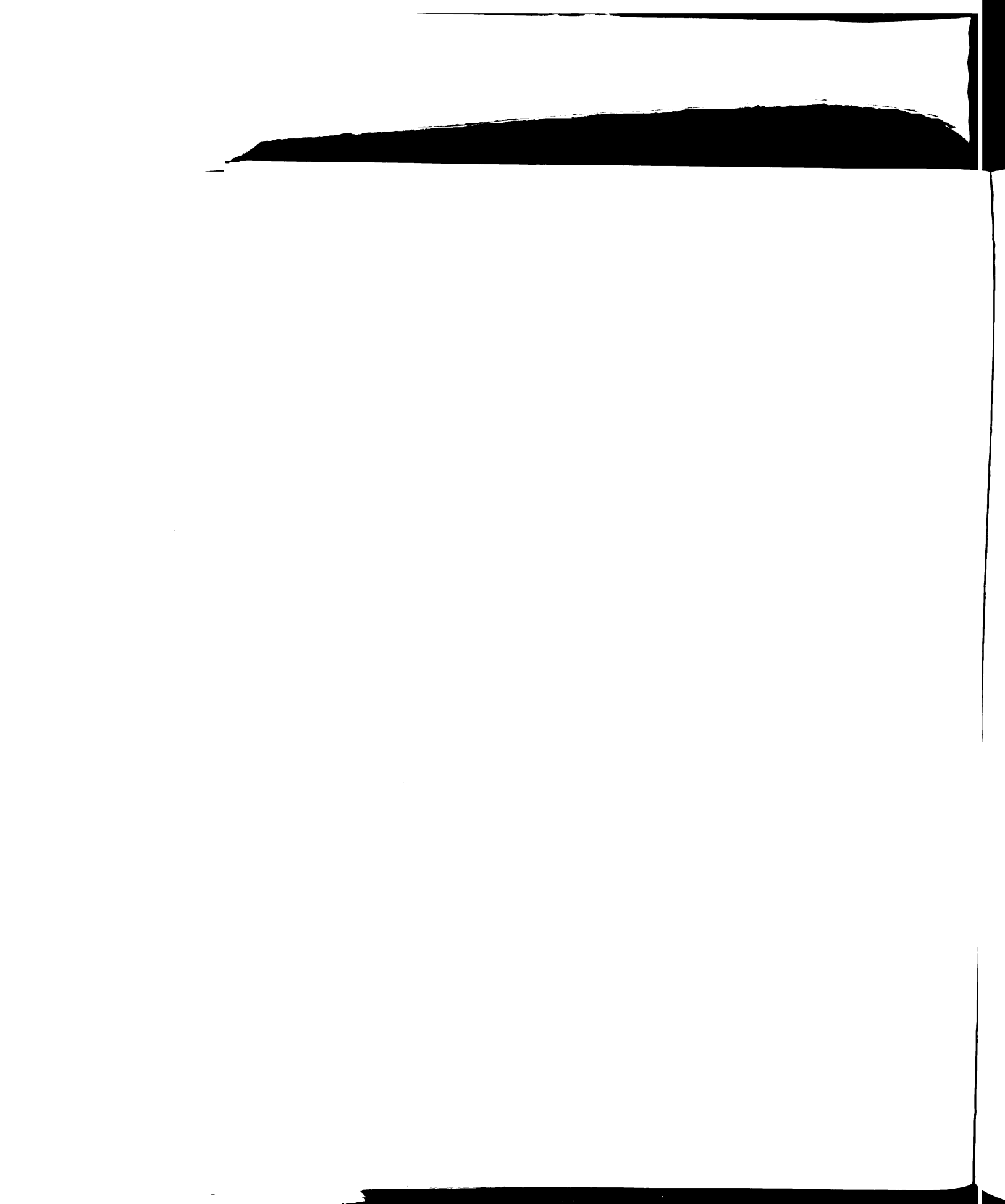

$$\frac{\dfrac{\partial f(M_i, S_i)}{\partial M_i}}{\dfrac{\partial (\alpha_p)_i}{\partial t}} = \frac{\dfrac{\partial f(M_i, S_i)}{\partial S_i}}{\dfrac{\partial (\beta_p)_i}{\partial t}} = (K_1)_i \qquad 2.13$$

in which $(\alpha_p)_i$ and $(\beta_p)_i$ are the plastic components of α_i and β_i, respectively.

It must be pointed out that the governing equations of the discrete model are spacewise discrete, but the linear and angular accelerations, $\ddot{y}_i$ and $\ddot{\phi}_i$, are continuous in the time dimension. Therefore, temporally continuous solutions of these equations could be sought. However, these equations, as discussed later, will be integrated herein numerically.

2.3. Boundary Conditions

In the use of the model, supports will be made to coincide with force points. However, in the prototype (continuous) problem, boundary conditions are not always given in terms of stress resultants. Thus, whenever a boundary condition is given in terms of displacement in the prototype problem, it is necessary to interpret this condition as a stress resultant condition for the model.

Since the stress resultants are directly related to the deformations of the moment and shear springs, the prototype

displacement conditions must be used to compute these deformations. As will be shown later, this can be done through geometry. But first, the following relations at a boundary point should be noted.

$$[y]_{model} = [y + \int_o^{\frac{h}{2}} \frac{\partial y_{shear}}{\partial x}]_{continuum} \qquad 2.14$$

$$[\phi]_{model} = [\phi + \int_o^{\frac{h}{2}} \frac{\partial \phi}{\partial x}\, dx]_{continuum} \qquad 2.15$$

If $y = 0$ for the continuous case, Equation 2.14 reduces to

$$[y]_{model} = [\int_o^{\frac{h}{2}} \frac{\partial y_{shear}}{\partial x}\, dx]_{continuum} \qquad 2.16$$

If $\phi = 0$ for the continuum, Equation 2.15 will yield

$$[\phi]_{model} = [\int_o^{\frac{h}{2}} \frac{\partial \phi}{\partial x}\, dx]_{continuum} \qquad 2.17$$

The usual types of boundary conditions can now be taken singly.

Simple Supports: The condition that moment vanishes is straightforward and needs no further remark. The other condition of vanishing (total) displacement for the prototype implies, by Equation 2.16, that the model will have some shear deformation at the support representing the shear deformation of the continuum

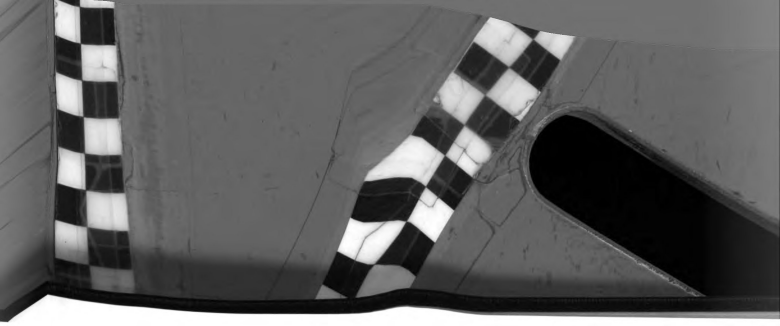

lumped from a tributary length of h/2 adjacent to the support. For the model, the value of this shear deformation can be determined from considerations of geometry.

If j (j=N+1) denotes a support at the right end of a beam, then the lumped shear deformations at the two ends of a simply supported beam are given by

$$\begin{aligned} \beta_1 &= y_1 - \frac{h_1}{2}\phi_1 \\ \beta_j &= -y_n - \frac{h_n}{2}\phi_n \end{aligned} \qquad 2.18$$

Knowing the deformation (or its increment), the shear force (or its increment) at the support can be computed.

Fixed Supports: In this case, Equation 2.17 gives the fixed end slope of a model as the lumped curvature due to bending, contributed by a length of h/2 adjacent to the support. From geometry, the rotations of the moment springs at the two fixed supports are given by

$$\begin{aligned} \alpha_1 &= \phi_1 \\ \alpha_j &= -\phi_n \end{aligned} \qquad 2.19$$

Knowing the rotation (or its increment), the moment (or its increment) at the support can be computed. Shears at fixed ends are found in precisely the same way as for simple supports.

Free Ends: Since both boundary conditions correspond to specifying stress resultants--moment and shear vanish--no special interpretations are necessary.

III. METHOD OF NUMERICAL SOLUTION

3.1. General

The method essentially consists of a step-by-step numerical integration of the system of equations presented in the foregoing chapter. The problem here may be formulated as follows: at some given time $t=t_o$, the system is known to be in an elastic state, and the values of all the displacements $y_i=y_i(t_o)$ (and $\phi_i = \phi_i(t_o)$) and their first derivatives $\dot{y}_i(t_o)$ (and $\dot{\phi}_i(t_o)$) are known. Furthermore, the external loading $P_i(t)$ is completely prescribed. It is required to determine the displacements and stress resultants at time $t_1=t_o+\Delta t$, where Δt is a small time increment.

For easy reference, the model presented earlier which contains the mechanism of shear deformation and rotatory inertia will be referred to as the "Timoshenko" model. Obviously, the model can be reduced to lesser forms. Thus, the "Shear" model refers to the case in which shear deformation is considered but rotatory inertia is neglected. The "Rotary" model refers to the case in which rotatory inertia is considered but shear deformation is neglected. Finally, when both effects are neglected, the model reduces to the "Euler" model.

The symbols T(N) will be used to denote: "Timoshenko model; beam divided into N equal panels." The symbols S(N),

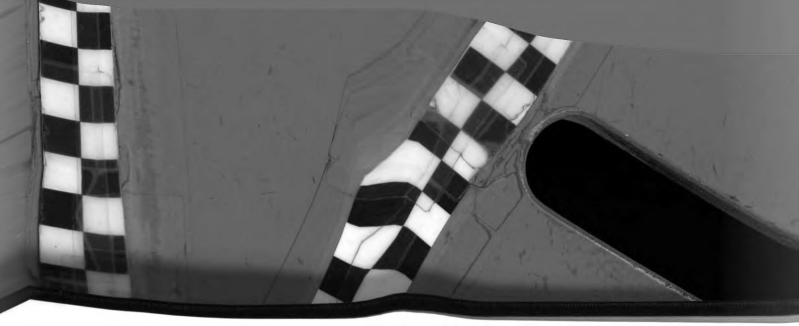

R(N), and E(N) are defined in a similar fashion. The analytical solution of the continuum case will be referred to as the "Exact" solution. The term "continuous beam" will be used to mean the continuum case; it does not refer to a multi-span beam structure, which is not treated here.

Theoretically, it is possible to obtain solutions of the "Shear," Rotary," and "Euler" models directly from the "Timoshenko" model. A solution of the "Shear" model could be obtained if the shear stiffness is taken as infinity. However, since this is not practical for numerical work, G may be assumed to be very large, thus letting the "Timoshenko" model approach the "Shear" model. Similarly, if the rotatory inertia term is taken close to zero, the "Rotary" model could be approached. By simultaneously using a large value for G and a small value for (ρ Ih) the "Euler" model can be approached.

This approach was not used here mainly due to technical difficulties. First, it is not clear how big or how small G and (ρ Ih) have to be in order to lead to satisfactory results; and secondly, the time increment needed for stability in the numerical integration has proven to be very sensitive to changes of these quantities (G and ρ Ih). In one instance, approaching the "Shear" model from the "Timoshenko" model required a time increment almost 10 times smaller than the "Shear" model requires.

In order to avoid these difficulties, it was found more convenient to develop the "Shear," "Rotary," and "Euler" models individually even though the numerical procedure of solution differs slightly from one model to another.

The procedure of solution for the different models will thus be described separately in the following. It should be noted that while the procedure is given for the "Timoshenko" model for both the elastic and the plastic range, for the other models, only the elastic case is considered.

3.2. The "Timoshenko" Model

Elastic Range

1. From geometry (see Figure 2.4), the initial ($t=t_o$) deformations of the shear and moment springs can be computed from known initial displacements (assuming ϕ to be sufficiently small):

$$\alpha_i(t_o) = \phi_i(t_o) - \phi_{i-1}(t_o) \qquad 3.1$$

$$\beta_i(t_o) = y_i(t_o) - y_{i-1}(t_o) - \frac{1}{2}\left(h_i\phi_i(t_o) + h_{i-1}\phi_{i-1}(t_o)\right) \qquad 3.2$$

2. So long as elasticity prevails, one can compute the moments $M_i(t_o)$ and shears $S_i(t_o)$ from Equations 2.10 and 2.11.

3. Knowing $M_i(t_o)$, $S_i(t_o)$, and the loading $P_i(t_o)$, the accelerations $\ddot{y}_i(t_o)$, and $\ddot{\phi}_i(t_o)$ can be computed from Equations 2.8 and 2.9, respectively. Thus, all quantities that enter into the problem are known for $t=t_o$.

4. The changes in the displacements at $t=t_1$ can now be determined by a forward numerical integration procedure. The

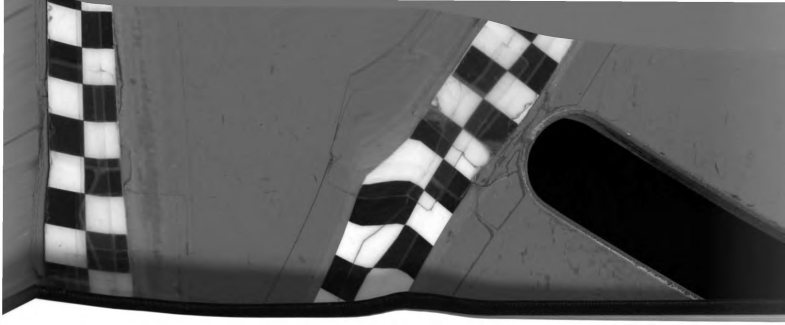

formula used in this thesis is:

$$y_i(t_1) = y_i(t_o) + (t_1 - t_o)\dot{y}_i(t_o) + \frac{1}{2}(t_1 - t_o)^2 \ddot{y}_i(t_o) \qquad 3.3$$

and similarly for $\phi_i(t_1)$ (see Reference 32).

5. Knowing the displacements, one goes through the same procedure as outlined in steps (1) through (3) and obtains $\ddot{y}_i(t_1)$ and $\ddot{\phi}_i(t_1)$.

6. The velocities at time t_1 can be computed by a numerical integration. The formula used here is

$$\dot{y}_i(t_1) = \dot{y}_i(t_o) + \frac{1}{2}(t_1 - t_o)(\ddot{y}_i(t_o) + \ddot{y}_i(t_1)) \qquad 3.4$$

and similarly for $\dot{\phi}_i(t_1)$.

7. Thus, one is ready to repeat the process to solve for the response at $t_2 = t_1 + \Delta t$, etc.

Elastic-Plastic Range

Successive applications of the cycle of integration in the elastic range will, at some time, yield values of M and S that violate the plastic potential theory; that is to say, f(M, S) will become positive. Smaller time increments will then be tried until a time τ_o is found when f(M, S) = 0 (within a prescribed degree of accuracy).

The numerical method, representing a finite incremental form of the plastic potential theory, is given below for one step of integration in the plastic region.

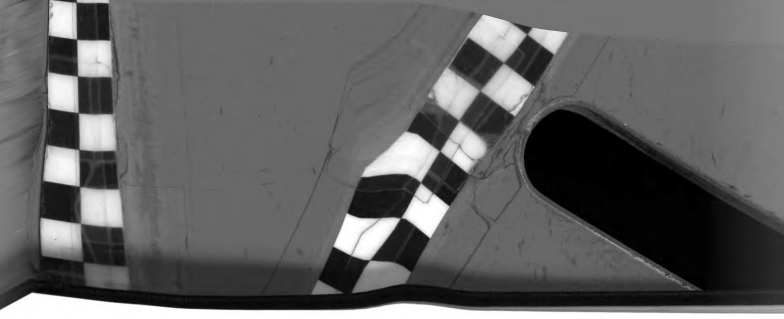

Let plasticity start at time $t_i = \tau_o$. Since Equations 3.1 through 3.3 apply, the increments $\Delta\alpha$ and $\Delta\beta$ are known for the next time increment $\Delta\tau_1$; however, the material property Equations 2.10 and 2.11 can not be applied to the whole of $\Delta\alpha$ and $\Delta\beta$. Therefore, the problem becomes one of splitting $\Delta\alpha$ and $\Delta\beta$ into elastic and plastic portions, of which $\Delta\alpha_e$ and $\Delta\beta_e$ (the elastic portions of $\Delta\alpha$ and $\Delta\beta$) will produce changes in the stress resultants, but the plastic portions, $\Delta\alpha_p$ and $\Delta\beta_p$ do not affect the stress resultants.

A graphical representation of the necessary technique is given in Figure 3.1 for a typical force point. The yield curve is not specified, indicating that the method is general, and it applies to any plastic potential function.

In Figure 3.1 the ordinate is assigned the dual scales of m (the non-dimensional moment M/M_y) and $\Delta\bar{\alpha}$ (the non-dimensional angle change $\Delta\alpha/\alpha_y$, where α_y is the change of rotation corresponding to a totally elastic change of moment $\Delta M = M_y$ at the particular force point). Similarly, the abscissa is assigned s ($s = S/S_y$) and $\Delta\bar{\beta}$ ($\Delta\bar{\beta} = \Delta\beta/\beta_y$, where β_y is the shear slide corresponding to a totally elastic change of shear $\Delta S = S_y$ at the force point). It is important to note that, this scaling has made possible a direct graphical correspondence betwen ΔM and $\Delta\alpha_e$, and similarly for shear.

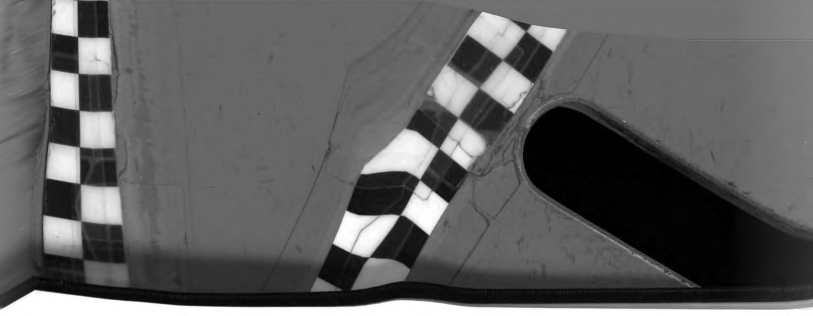

Let A (Figure 3.1) be the position of the stress state at time τ_o. The vector d (with components $\Delta\bar{\alpha}$, $\Delta\bar{\beta}$) is laid on the graph with its tail at A (AD). Next, a circle is constructed with AD as a diameter to intersect the yield curve at B (and of course, A). Then, B is the stress state at time $\tau_o + \Delta\tau_1$. Moments and shears are read directly from the graph at point B. Furthermore, the components of AB on the $\Delta\bar{\alpha}$ and $\Delta\bar{\beta}$ scales are the elastic parts of these quantities. The components of BD (the perpendicular to AB) are the plastic parts of $\Delta\bar{\alpha}$ and $\Delta\bar{\beta}$. The validity of the preceding statements is explained in the following.

There are three conditions to be satisfied by the division of $\Delta\alpha$ and $\Delta\beta$ into the elastic and plastic parts. First,

$$\begin{aligned} \Delta\alpha &= \Delta\alpha_e + \Delta\alpha_p \\ \Delta\beta &= \Delta\beta_e + \Delta\beta_p \end{aligned} \qquad 3.5$$

secondly, the new stress state at time $\tau_o+\Delta\tau_1$ computed from $\Delta\alpha_e$ and $\Delta\beta_e$ (using Equations 2.10 and 2.11) must satisfy the yield condition, i.e., Equation 2.12; and thirdly, the plastic flow rate vector must be normal to the yield curve (Equation 2.13).

The first condition is satisfied here from simple geometry considerations. The second one is obviously satisfied since point B is on the yield curve. As for the third, since Figure 3.1 is constructed for a very small time interval, the vector quantities $\Delta\bar{\alpha}_p$ and $\Delta\bar{\beta}_p$ essentially represent the rates of the plastic

deformations. Therefore, the flow rule of Equation 2.13 is satisfied on a finite increment basis.

When the vector AD points inward, elasticity is resumed and Equations 2.10 and 2.11 are validated for the whole of $\Delta\alpha$ and $\Delta\beta$. It must be noted that, while one or more force points may go plastic and require the treatment described above, other points that remain elastic will, or course, be handled according to the elastic rules.

Conceptually, the graphical procedure outlined above is simple and straightforward. However, the programming of it on a computer, though feasible, is not convenient. Therefore, to facilitate programming, the further assumptions are made that the arc AB can be approximated by a circle whose curvature, and center of curvature are those of the actual yield curve at point A, as shown in Figure 3.1. Since the length AD can be controlled by the size of $\Delta\tau$, the error introduced due to the above approximation can be kept as small as needed by using a sufficiently small $\Delta\tau$. The method is, in general, consistent with the forward integration method used throughout this study. Note that, so far as the flow rule of Equation 2.13 is concerned, the procedure incurs no error except that of approximating an arc by a chord, which is inherent in the numerical integration method.

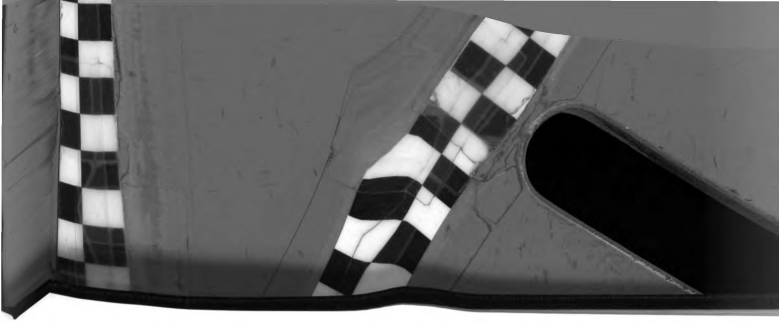

3.3. The "Shear" Model

The "Shear" model differs from the "Timoshenko" model in that the rotatory inertia is neglected. Thus Equation 2.9 assumes the form

$$0 = M_i - M_{i+1} + \frac{h_i}{2}(S_i + S_{i+1}) \qquad 3.6$$

In case of the "Timoshenko" model both y_i and ϕ_i are independent quantities. For the "Shear" model they are not independent and the relationship is to be obtained as follows:

a) By substituting β_i's from Equations 3.2, Equations 2.11 are written out for S_i in terms of y_i and ϕ_i.

b) Equations 2.10 are written out for M_i in terms of ϕ_i.

c) The expressions for shear from (a) and the expressions for moment from (b) are then related by Equation 3.6. Thus the following relationship between ϕ_i and y_i is obtained (taking h_i=h for all i):

$$\begin{aligned}
&(b)\ \phi_1 + (-1 + \frac{K_2 h}{2})\phi_2 && = K_2 y_2 + K_2 y_1 \\
&(-1 + \frac{K_2 h}{2})\phi_1 + (2 + \frac{K_2 h}{2})\phi_2 + (-1 + \frac{K_2 h}{2})\phi_3 && = K_2 y_3 - K_2 y_1 \\
&\quad\vdots \\
&(-1 + \frac{K_2 h}{2})\phi_{n-1} + (b)\,\phi_n && = -K_2 y_{n-1} - K_2 y_n
\end{aligned} \qquad 3.7$$

where $K_2 = \frac{k'AGh}{2EI}$; b depends on the boundary conditions, for

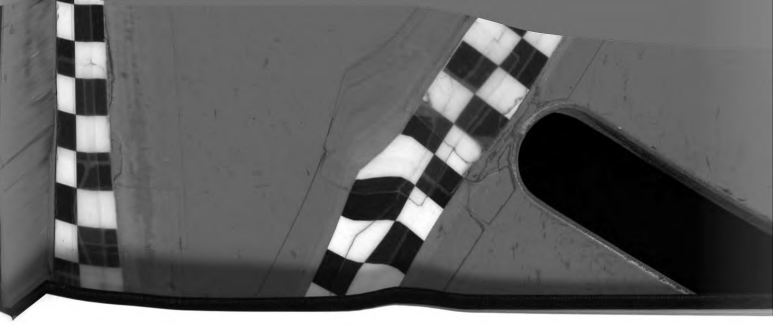

simple supports $b=1+1.5K_2h$, for fixed supports $b=3+1.5K_2h$. The second equation from the top is typical.

Except for the step that ϕ_i's are obtained from Equation 3.7 (instead of by numerical integration) the numerical procedure for the "Shear" model is the same as the one outlined in Section 3.2 for the "Timoshenko" model.

3.4. The "Rotary" and "Euler" Models

The "Rotary" model differs from the "Timoshenko" model in that the shear deformation is neglected. Hence, the displacement of the "Rotary" model does not exhibit any jumps due to shear. Consequently, for a beam with N panels, there can be only N-1 independent displacements y_i. Similarly, all ϕ_i's are fixed by geometry once the y_i's are determined.

The supplementary geometry equations may be taken as,

$$y_n = y_{n-1} - y_{n-2} + y_{n-3} - \cdots \qquad 3.8$$

and, by setting $\beta_i = 0$ in Equation 3.2 and solving, one obtains,

$$\begin{aligned} \phi_i &= \frac{1}{h}(2y_i - 4y_{i-1} + 4y_{i-2} \cdots .) \\ \phi_n &= -\frac{2y_n}{h} \end{aligned} \qquad 3.9$$

The numerical procedure for this case differs from that for the "Timoshenko" model in another aspect. Since $\beta_i = 0$ and $G = \infty$ Equation 2.11 can no longer be applied to calculate the shears which are now governed only by the kinetic equations.

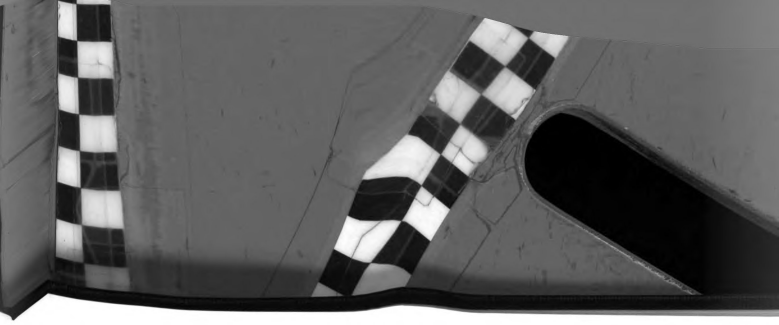

Using Equations 3.8 and 3.9, Equations 2.8 and 2.9 can be combined to eliminate all the second time derivatives so that the shears $S_1, \ldots S_n$ are related only to the bending moments and the external loads. (Note that the moments are computed from Equation 2.10 as previously.)

The resulting system of equations appears as,

$$\begin{bmatrix} 1+K_3 & 1-K_3 & 0 & 0 & & & \\ -2K_3 & 1+3K_3 & 1-K_3 & 0 & 0 & & \\ 2K_3 & -4K_3 & 1+3K_3 & 1-K_3 & 0 & 0 & \\ -2K_3 & +4K_3 & -4K_3 & 1+3K_3 & 1-K_3 & 0 & \\ \cdot & & & & & & \\ \cdot & & & & & & \\ \pm(1+K_3) & \cdots & \cdots & -2-2K_3 & 2+2K_3 & -2-2K_3 & 3+K_3 \end{bmatrix} \begin{bmatrix} S_1 \\ S_2 \\ \cdot \\ \cdot \\ \cdot \\ \cdot \\ S_n \end{bmatrix} = \begin{bmatrix} C_1 \\ C_2 \\ \cdot \\ \cdot \\ \cdot \\ \cdot \\ C_n \end{bmatrix} \qquad 3.10$$

where $K_3 = \frac{4(\rho I h)}{m h^2}$ by taking equal h_i's. A typical C_i is given by

$$C_i = K_3 P_i - 2K_3 P_{i-1} + 2K_3 P_{i-2} - \cdots - \frac{2}{h}(M_i - M_{i+1})$$

but

$$C_n = P_n - (1 + K_3) P_{n-1} + (1 + K_3) P_{n-2} - \cdots - \frac{2}{h}(M_n - M_j)$$

The set of simultaneous Equations 3.10 are solved to obtain the shears. The shear at the last force point, S_j, is obtained from Equation 2.7. The shears can now be used in Equation 2.8 to calculate $\ddot{y}_i$ which are, in turn, used to compute the displacements

y_i for the next time interval. The cycle is then completed.

The "Euler" model differs from the "Rotary" model in that the rotatory inertia is neglected. The numerical procedure is the same as that for the "Rotary" model except that, in arriving at Equation 3.10, Equation 3.6 is used instead of Equation 2.9.

3.5. Time Increment

Mathematically, the method used here is analogous to a numerical integration of a system of partial differential equations which are, in general, nonlinear. The size of the time increment for each step of integration obviously plays a dominant role.

Unfortunately, there seems to be no rigorous method in existence of estimating the appropriate values of Δt to use. A trial method, therefore, was used to determine a satisfactory time increment. The following is a conservative listing of the time increments in terms of T_1, which is numerically equal to the fundamental period of vibration of a simply supported, elastic continuous Euler beam.

a) "Timoshenko" and "Shear" models:

$\Delta t = \frac{1}{5} \frac{T_1}{N^2}$ for I-sections and all values of N; for N > 20, Δt can be based on N = 20.

$\Delta t = \frac{1}{10} \frac{T_1}{N^2}$ for rectangular cross-sections and all values of N.

b) "Rotary" and "Euler" models:

$$\Delta t = \frac{1}{10}\,\frac{T_1}{N^2} \quad \text{or} \quad \Delta t = \frac{T_1}{N^3} \quad \text{whichever is smaller.}$$

It must be emphasized that the preceding is based on the numerical experience of the present study which has dealt with a rather simple kind of loading. The above listing may not apply if the loading is substantially different.

3.6. Use of the Computer

The computer work for this study was conducted on the digital computer CDC3600 at Michigan State University. The Fortran language was used.

It is found that the time of compilation, loading, etc., is about one minute. For N = 10 and for a length of time $t = 3T_1$ the execution of the program takes somewhat less than a minute. For the problems solved, the maxima are usually reached at $t < 0.5T_1$ (but it may be necessary to carry the solution as far as $t = 3T_1$ in order to estimate the permanent set).

For larger values of N, the time needed is slightly more than that calculated according to the square of the ratios of N.

The time corresponding to the "Shear," "Rotary," and "Euler" models can be estimated using the information given in Section 3.4.

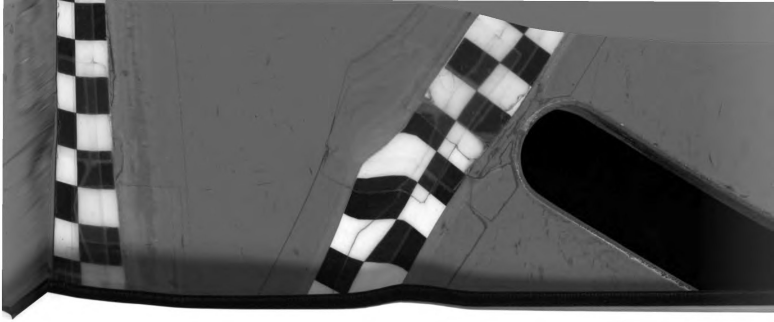

IV. RESULTS IN THE ELASTIC RANGE

4.1. Introduction

The results presented in this chapter deal exclusively with response in the elastic range. The convergence of mid-span moments, end shears, and maximum deflections are shown for the four models considered here. Also investigated is the relative importance of shear and rotatory inertia in elastic vibrations.

According to the notations in Figure 4.1 the example beam has the following cross-sectional dimensions: B = 5", H = 6", $\bar{t}_w = 0.0346$, T = 0.577. The beam is simply supported at both ends, and divided into panels of equal length. Except for the data presented in Section 4.4, the length of the beam is 10 ft.

A blast type loading, applied uniformly on the beam, is given by the expression

$$w(x, t) = cW\, e^{-2t/T_1} \qquad 4.1$$

where c is a parameter representing the load intensity, and $W = 8M_y/L^2$ is the load necessary to cause yield in the mid-span of the beam.

4.2. Convergence of the "Euler" Model

The "Euler" model is the simplest of all the models studied.

In fact, it can be considered to be a special case of each of the other models. For this model, an exact analytical solution is obtainable, and can rightly be regarded as the true limit to which the discrete model should converge. Strictly speaking, the convergence to the true limit of a special case does not necessarily imply similar convergence of more general cases. However, it should certainly strengthen the case for the other models (for which there are no exact analytical solutions available for comparison). It is essentially in this regard that the study of the convergence of the "Euler" model is significant for the purpose of the present work.

The "Exact" solutions (see Appendix), as well as the "Euler" model solutions for various values of N are plotted in Figures 4.2, 4.3, 4.4 for the center deflection, center moment, and end shear, respectively. (The deflections are scaled by Y_y, the maximum static deflection.). For more precise comparisons, the values of the maximum responses and their times of occurrence are also noted in the figures. As expected, the deflection converges to the "Exact" solution considerably faster than the moment and the shear. For N = 21, the deflection is so close to the exact solution that they are represented by a single curve in Figure 4.2. (That odd number of panels is necessary for mid-span deflection is a consequence of the

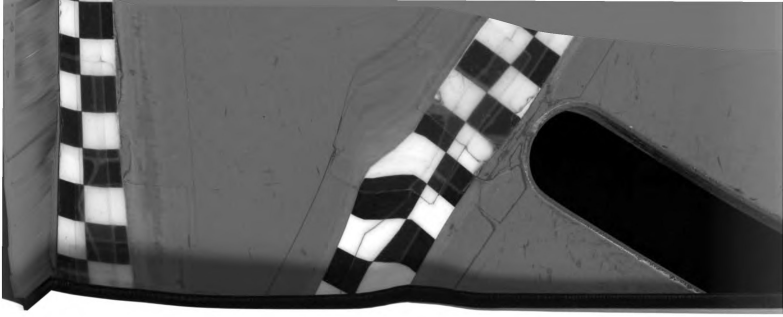

construction of the model: the deflections are defined only at mass points, and the supports are made to coincide with force points; see Chapter II.) For N = 20 the moment values still have noticeable differences from the "Exact" curve at some intervals. Although the exact maximum moment is approximated well even by using the small value of N = 4, it is important to note that the comparison should be viewed for the entire range of response. Thus, it is seen that overall agreement increases with larger values of N.

The preceding is also generally true for end shear. In order not to clutter the illustration, shear responses are shown in Figure 4.4 only for N = 10 and the exact solution. The agreement is seen to be good, and it improves with larger values of N (not shown).

4.3. "Apparent" Convergence of the "Rotary," "Shear," and "Timoshenko" Models

Since exact analytical solutions for the limiting cases ($N = \infty$) of these models are not available, the "convergence" is considered by comparing numerical results using different values of N.

Results for the "Rotary" model are shown in Figures 4.5, 4.6, and 4.7 for deflections, moments, and shears. Results for the "Shear" model are shown in Figures 4.8, 4.9, and 4.10 for the same quantities. Data illustrating the apparent convergence of the "Timoshenko" model are presented in Figures 4.11, 4.12, and 4.13,

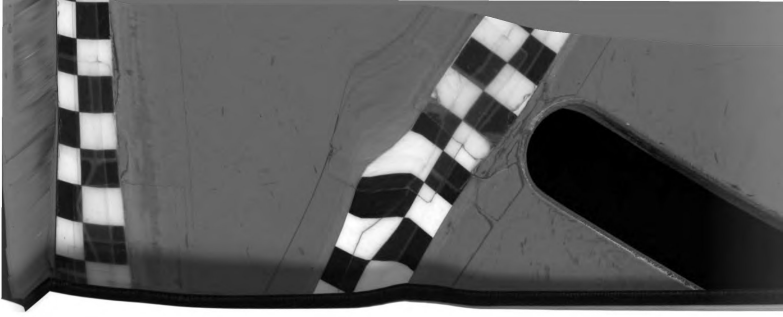

respectively, for deflection, moment, and shear. From an examination of all these data it may be reasonably concluded that the results converge to some limit, and are trustworthy.

From a comparison of the shear responses by the "Rotary" and "Shear" models (see Figures 4. 7 and 4. 10) it is of interest to note that by considering shear deformations the shear response becomes appreciably smoother.

4. 4. Relative Importance of Shear and Rotatory Inertia

A comparison of the moment and shear response curves presented in the preceding sections will show that neither the maximum moment nor the maximum shear varies appreciably from one model to the other. Particularly, the maximum stresses shown by the "Rotary" model and the "Euler" model are well within 1% of each other, whereas the "Shear" and "Timoshenko" models exhibit almost identical behavior in all cases.

This is illustrated, for the moment, in Figure 4. 14. The differences between the "Rotary" and "Euler" models or between the "Timoshenko" and "Shear" models represent the influence of the rotatory inertia. It is seen that this influence is small indeed. The differences between the "Shear" and "Euler" models or between the "Timoshenko" and "Rotary" models represent the influence of shear deformations. This influence is seen to be appreciable.

The preceding data pertain to a beam with a 10 ft. span. Additional data for shorter spans are presented in Figure 4. 15 for considerations of the effects of rotatory inertia and shear deformations. All curves plotted in the figures represent the differences between the results given by the discrete models (N = 10) and those corresponding to an exact solution of the continuous Euler beam.

As expected, the influence of shear deformations on deflections is to increase the deflections with decreasing span length. The effect of the shear deformations is to decrease both the midspan moment and end shear. For moment, the reduction stays essentially constant for span length greater than 6 ft. For shorter spans, the reduction increases. The shear reduction exhibits an oscillatory pattern.

The differences between the pairs of graphs are obviously due to rotatory inertia. It is seen that the qualitative effects of rotatory inertia are to decrease the deflection and the moment, but to increase the end shear. However, the magnitudes of these effects are very small.

In addition to the preceding, a number of beams with different cross-sectional properties and lengths were also solved to see whether the contributions due to rotatory inertia could be significant. It was found that neither the stresses nor deflections were affected appreciably by rotatory inertia. Hence, the data are not presented herein.

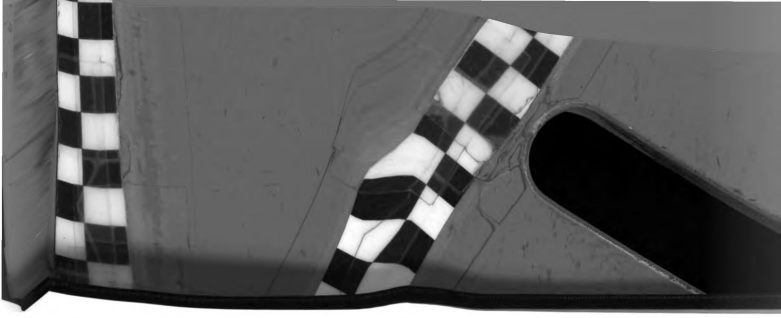

V. ELASTIC-PLASTIC BEHAVIOR OF THE "TIMOSHENKO" MODEL

5.1. Introduction

In this chapter, the apparent convergence of the elastic-plastic response of the "Timoshenko" model is considered first. Then, the inelastic behavior of simply supported and fixed-fixed I-beams is studied. The parameters considered are the web thickness and the span length. The variables are the maximum deflection, permanent set (permanent total deflection), and permanent shear slide.

Except for varying length or web thickness, the beams analyzed in this chapter are generally the same as described in Section 4.1. The ranges of the parameters are, in the notation of Figure 4.1, $0.2 > \bar{t}_w > 0.025$, and $6' < L < 20'$.

The loading used is the same as given by Equation 4.1. However, the parameter c is set equal to unity in order to carry the problem into the plastic range. Furthermore, after all the maximum responses have been reached, and elasticity resumed, the external loading is removed in order to obtain the permanent set from the subsequent free vibration.

As described in Chapter II, for an analysis in the plastic range, it is necessary to define a yield or interaction curve. (This cross-sectional property will be generalized for the discrete model

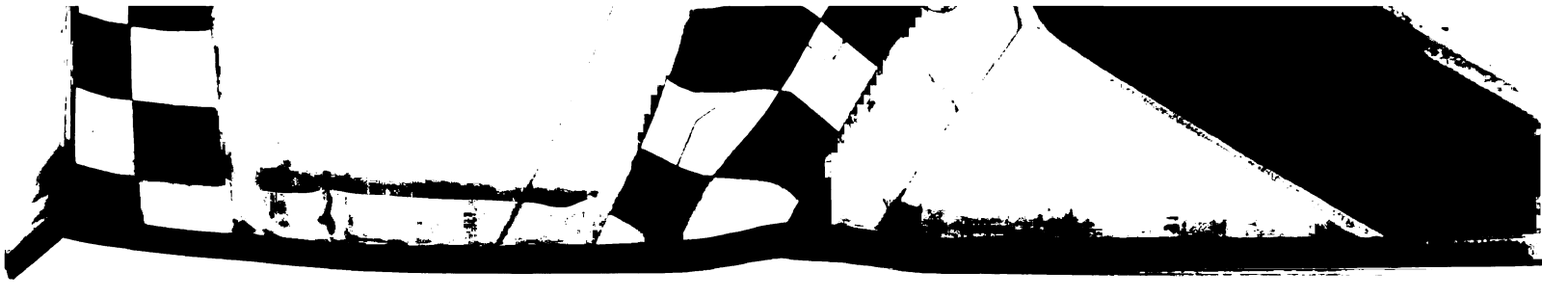

as a discrete joint property.) Though a considerable amount of theoretical work has been reported on this subject (13, 19, 25, 29, 30, 31), experimental data is very scarce (9, 15). For the numerical work here, two yield curves will be used:

$$m^{12} + s^2 = 1 \qquad 5.1$$

$$m^2 + s^2 = 1 \qquad 5.2$$

where m and s are, respectively, the non-dimensional moment M/M_y, and shear S/S_y. The moment capacity, M_y, is computed for the cross-section by assuming that the whole section has yielded at ±33000 psi. The shear capacity, S_y, is obtained as k'A (the "active shear area") times the shear yield stress, taken to be 18000 psi.

The relationship of Equation 5.1 may be regarded as a good approximation to the actual behavior of I-sections, and agrees well with certain relationships which were formulated with some experimental basis (9, 15). On the other hand, Equation 5.2 underestimates the strength of the section; thus, it should be considered to be a lower bound. Figure 5.1 illustrates the interaction relationships of Equations 5.1, 5.2, and the one given in Reference 9.

5.2. Convergence of the "Timoshenko" Model in the Elastic-Plastic Range

In Chapter IV the convergence of the "Timoshenko" model in the elastic range was shown. Here, an elastic-plastic example is

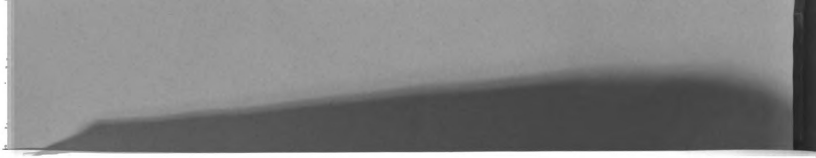

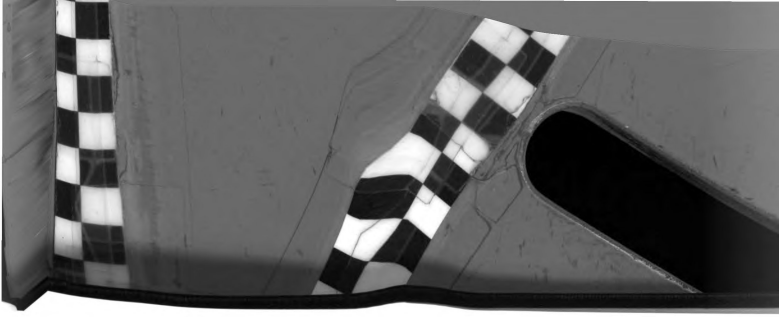

treated. The beam is a 12WF53 (I-beam), 10 ft. long, and fixed at the ends. The yield criterion of Equation 5.2 is assumed.

As before, the deflection converges very rapidly, therefore, it is not presented. The moment and the shear at the support are plotted, respectively, in Figures 5.2 and 5.3 for several values of N.

In the case of the moment, N = 20 and N = 40 give results that are very close to each other. As for the shear, one may note that the convergence is even more satisfactory than for the elastic case! (Compare Figures 4.10 and 5.3.) (Seemingly, plastic yielding serves to attenuate the higher modes' effects.)

It is of interest to trace the locus of the stress state of the elastic-plastic response. This is shown in Figure 5.4. Numerals on the locus correspond to those times similarly noted in Figures 5.2 and 5.3. Of course, the ranges between points (3), (4), and (5) are plastic, while the rest of the locus is elastic.

5.3. Response of Simply Supported I-Beams with Different Lengths and Web Thicknesses

It is reasonable to expect that, for shorter beams, yielding would start first at the supports, then spread toward the mid-span. For longer beams, yielding would start at the mid-span, then spread outward. This behavior is illustrated in Figure 5.5 for beams with

constant non-dimensional web thickness $\bar{t}_w = 0.0346$ but with spans varied from 6 ft upwards. The yield curve of Equation 5.2 is used. Further dividing lines are placed in this figure to show the degree of interaction. (For instance, the region between the 80% and 95% lines, has yielded at values of maximum shear that are only 80% to 95% of the shear capacity. This is, of course, caused by the small amount of moment present in this region.)

In Figure 5.6 are plotted, for the same parameters as above, the maximum deflection, the permanent set, and the permanent slide. Full lines correspond to the data obtained by use of Equation 5.2 as the yield curve; dotted lines correspond to Equation 5.1.

It is noted that the displacements are scaled by the maximum (elastic) static deflection. For the present set of parameters, the elastic-plastic "Euler" model gives the maximum non-dimensional deflection as a constant equal to 1.56 for all span lengths. (Indeed, the choice of the external loading and the scaling of the deflections are responsible for this constancy.) Therefore, it is apparent that the difference between the maximum deflection curves and the constant "Euler" solution is entirely due to the effects being considered here: rotatory inertia, and shear. (The latter, of course, is mostly responsible for the difference.) For longer beams, the maximum deflection curves are seen to approach the "Euler" case, indicating that shear and rotatory inertia effects become less important.

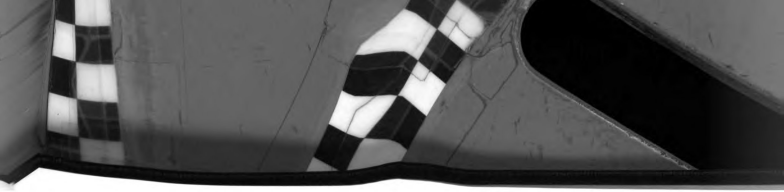

A similar observation can be made for the permanent set curve. Although the numerical data from the "Euler" solution have not been obtained, it is seen that for longer beams increasing the length did not change the essentially constant behavior of the sets. Also, as expected, the permanent slide converges to zero as the beam length is increased. On the other hand, as the beam becomes shorter, the permanent slide constitutes a higher portion of the permanent set.

It is seen that the two yield criteria used give results that show little difference from each other. This can be explained by the fact that, for simply supported beams, yielding is dominated by either moment (mid-span region) or shear (support region). For these stress conditions the two yield curves used are quite close (see Figure 5. 1).

Figure 5. 7 shows a set of curves similar to those just discussed. In this case, the beam length is held constant at 10 ft, and the web thickness is varied. It is seen that these curves have shapes similar to those in the previous figure. Recognizing that, so far as shear effects are concerned, a decrease in span length has the same qualitative effect as a decrease in web thickness, one can make observations about these data analogous to those made in connection with the preceding figure. It may be noted that, in this case, most structural I-beams, except for those with very thin webs,

are not greatly affected by shear, if they are simply supported. In the following section, it is shown that such is not the case for fixed-fixed beams.

5.4. Response of Fixed-Fixed I-Beams with Different Lengths and Web Thicknesses

A feature of fixed-fixed beams is that, at the supports both moment and shear can be large and thus strong interaction would take place in the plastic response.

The moment and shear forces at the fixed end are shown in Figure 5.8 for an I-beam with $\bar{t}_w = 0.0346$ and a varying length (as marked on the curves). The yield curve of Equation 5.2 is used. It is seen that for longer beams yielding takes place due to relatively higher values of the moment; for shorter beams yielding is mostly due to shear.

This is further illustrated in Figure 5.9 which shows the maximum deflections, permanent sets, and permanent slides. Unlike simply supported beams (see Figure 5.6), the results corresponding to the two interaction curves are quite distinct. This can be explained by referring to Figure 5.1 and noting that there is an appreciable difference between the two yield curves in the region where both moment and shear play a substantial role.

In Figure 5.10 the maximum deflection, permanent set, and permanent slides are presented for a constant length of 10 ft and

varying web thickness. Together with the results shown in Figure 5.9, the graphs in Figure 5.10 indicate that, similar to the case of the simply supported beams, as the span length or web thickness is increased, the response curves seem to level off, indicating a decrease in the shear (and some rotatory inertia) effects and an approach to the "Euler" case. On the other hand, Figure 5.10 indicates that at a length of 10 ft, most I-beams are very sensitive to shear effects.

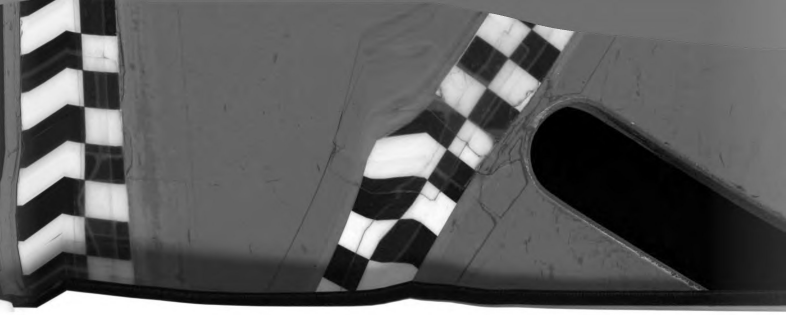

VI. CONCLUSION

In this thesis a method of analysis of the elastic-plastic vibrations of beams has been presented. The analysis has included the effects of shear deformations, rotatory inertia, as well as the interaction of moment and shear forces on the yield behavior.

The method employs a discrete physical model. This, together with the use of a numerical procedure, makes it possible to handle beams with different loading and boundary conditions which have, in general, limited the practicality of the continuum approach to this type of problems.

In the absence of exact analytical solutions, the reliability of the model is established essentially empirically by the "apparent convergence" of the deflections, moments, and shears, as the beam is divided into larger numbers of panels. (An exception is the "Euler" model in the elastic range, which has yielded solutions that converge to an exact analytical solution.)

Extensive numerical results have been obtained to study the influence of the web thickness and span length of I-beams on the relative importance of shear deformation. It is shown that as the length (or web thickness) is increased, results given by the "Timoshenko" model converge to that of the (elastic-plastic) "Euler"

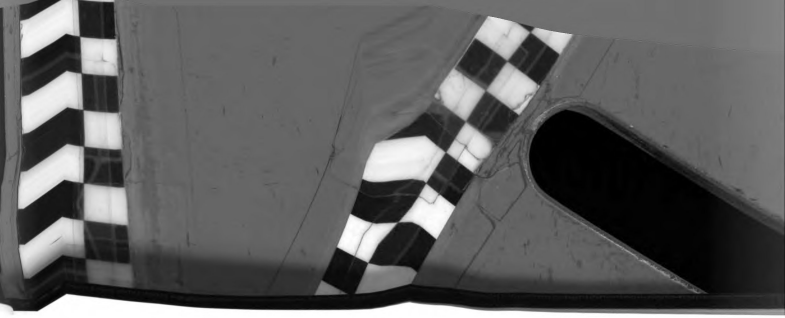

model. As expected, this analysis indicates that shear and rotatory inertia effects become negligible for longer (or thicker webbed) beams. However, it is also shown that the shear effects are substantial, and hence should be considered, even for beams of quite usual proportions. For example, for a 10 ft. long simple span (typical I-section), the permanent shear slide accounts for 35% of the total permanent displacement. The percentage could be much higher, depending on the form of the interaction curve, if the beam is fixed at the ends. It is further indicated that the interactions between shear and moment on the yield behavior play a significant role in the inelastic response. This is particularly true for beams with fixed ends.

From experience gained in the numerical work of this investigation, the following observation regarding the relative merits of the different models considered herein is noteworthy: The efficiency of a model seems to improve as its number of degrees of freedom (for equal values of N) is increased. Thus, the "Timoshenko" model is seen to converge the fastest, that is, it yields sufficiently accurate results for lower values of N and for larger values of the time increment! Consequently, it is concluded that, even in the elastic range and when shear and rotatory inertia effects are not sought, the "Timoshenko" model will yield more accurate results with less computer time.

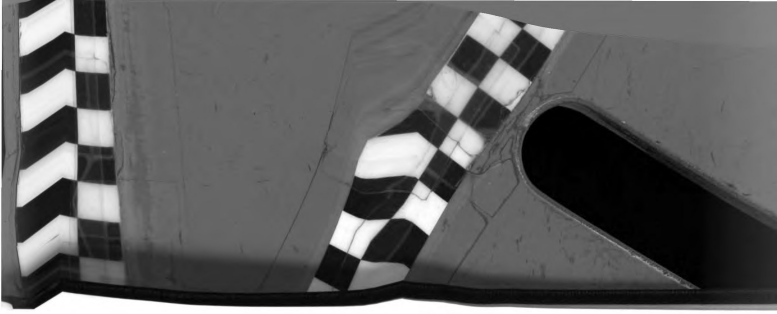

As possible items of future work on the subject, it is suggested that experiments be carried out so that the validity of the method of analysis could be examined. So far as the theory is concerned, it seems feasible that the method of analysis could be extended to consider the strain hardening case. Finally, a more rigorous mathematical treatment of the choice of the time increment in the integration procedure for the problems considered here should prove worth while.

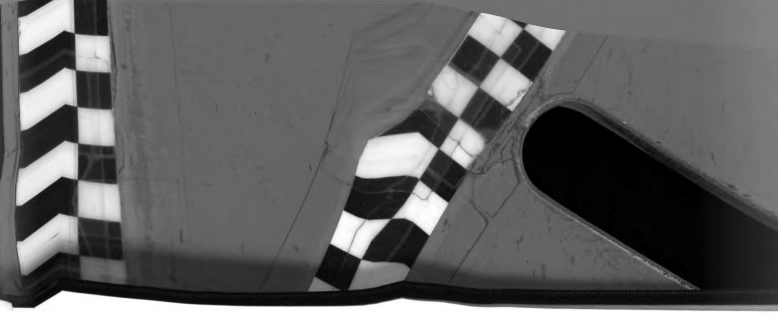

BIBLIOGRAPHY

1. Anderson, R. A. "Flexural Vibrations in Uniform Beams According to the Timoshenko Theory," Journal of Applied Mechanics, Vol. 20, No. 4, December 1953.

2. Archer, S. S. "Consistent Mass Matrix for Distributed Mass Systems," Journal of the Structural Division, Proc. of the ASCE, Vol. 89, Part 1, August 1963.

3. Baron, M. L., Bleich, H. H. and Weidlinger, P. "Dynamic Elasto-Plastic Analysis of Structures," Journal of Engineering Mechanics Division, Proc. of the ASCE, Vol. 87, No. EM1, February 1961.

4. Berger, B. S. "Dynamic Response Functions," Journal of the Engineering Mechanics Division, Proc. of the ASCE, Vol. 90, No. EM4, August 1964.

5. Bleich, H. H. and Shaw, R. "Dominance of Shear Stresses in Early Stages of Impulsive Motion of Beams," Journal of Applied Mechanics, Vol. 27, No. 1, March 1960.

6. Bodner, S. R. and Symonds, P. S. "Experimental and Theoretical Investigation of the Plastic Deformation of Cantilever Beams Subjected to Impulsive Loading," Journal of Applied Mechanics, Vol. 29, No. 4, December 1962.

7. Boley, B. A. and Chao, Chi-Chang, "Timoshenko Beams Under Dynamic Loads," Journal of Applied Mechanics, Vol. 25, No. 1, March 1958.

8. Bresse, M. "Cours de Mecanique Appliquée," Mallet-Bachelier, 1859.

9. Cooper, P. B., Lew, H. S., and Yen, B. T. "Welded Constructional Alloy Steel Plate Girders," Journal of the Structural Division, Proc. of the ASCE, Vol. 90, No. ST1, Part 1, February 1964.

10. Crandall, S. H. "The Timoshenko Beam on an Elastic Foundation," Proc. of the Third Midwestern Conference on Solid Mechanics, Ann Arbor, Michigan, 1957.

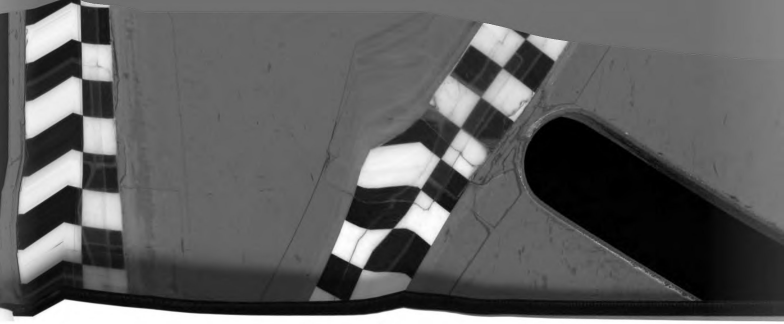

11. Das, S. K. "Rotatory Inertia Effects of Attached Masses on the Vibration Frequencies of Beams and Plates," Doctoral Dissertation, Department of Applied Mechanics, Michigan State University, 1962.

12. Dengler, M. A. and Goland, M. "Transverse Impact of Long Beams, Including Rotatory Inertia and Shear Effects," Proc. of the First U. S. National Congress of Applied Mechanics, 1951, ASME, New York, N. Y., 1952.

13. Drucker, D. C. "Effect of Shear on Plastic Bending of Beams," Journal of Applied Mechanics, Vol. 23, No. 4, December 1956.

14. Fettis, H. E. "Some Simplifications in the Treatment of Rotary Inertia Effects for Transverse Vibration of Beams," Journal of Aerospace Sciences, Vol. 28, No. 3, March 1961.

15. Frost, R. W. and Schilling, C. G. "Behavior of Hybrid Beams Subjected to Static Loads," Journal of the Structural Division, Proc. of the ASCE, Vol. 90, No. ST3, Part 1, June 1964.

16. Harper, G. N., Ang, A. and Newmark, N. M. "A Numerical Procedure for the Analysis of Contained Plastic Flow Problems," Civil Engineering Studies, Structural Research Series No. 266, University of Illinois, Urbana, Ill., June 1963.

17. Herrmann, G. "Forced Motions of Timoshenko Beams," Journal of Applied Mechanics, Vol. 22, No. 1, March 1955.

18. Hill, R. "The Mathematical Theory of Plasticity," The Oxford Engineering Science Series, London 1950.

19. Hodge, P. G. "Plastic Analysis of Structures," McGraw-Hill Book Co., N. Y., 1959.

20. Huang, T. C. "The Effect of Rotary Inertia and of Shear Deformation on the Frequency and Normal Mode Equations of Uniform Beams with Simple End Conditions," Journal of Applied Mechanics, Vol. 28, No. 4, December 1961.

21. Jones, R. P. N. "The Wave Method for Solving Flexural Vibration Problems," Journal of Applied Mechanics, Vol. 21, No. 1, March 1954.

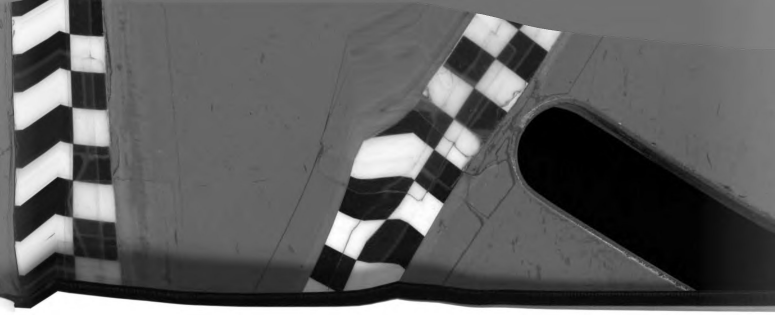

22. Karunes, B. and Onat, E. "On the Effect of Shear on Plastic Deformation of Beams Under Transverse Impact Loading," Journal of Applied Mechanics, Vol. 27, No. 1, March 1960.

23. Leckie, F. A. and Lindberg, G. M. "The Effect of Lumped Parameters on Beam Frequencies," The Aeronautical Quarterly, Vol. 14, Part 3, August 1963.

24. Lindberg, G. M. "Vibrations of Non-Uniform Beams," The Aeronautical Quarterly, Vol. 14, Part 4, November 1963.

25. Lu, Le-Wu "Linearized Interaction Curves for Plastic Beams Under Combined Bending and Twisting," AIAA Journal, Vol. 1, No. 3, March 1963, Technical Notes and Comments.

26. Luthe-Garcia, R., Walker, W. H. and Veletsos, A. S. "Dynamic Response of Simple-Span Highway Bridges in the Inelastic Range," Civil Engineering Studies, Structural Research Series, No. 287, University of Illinois, Urbana, Ill., December 1964.

27. Miklowitz, J. "Flexural Wave Solutions of Coupled Equations Representing the More Exact Theory of Bending," Journal of Applied Mechanics, Vol. 20, No. 4, December 1953.

28. Mindlin, R. D. and Deresiewicz, H. "Timoshenko's Shear Coefficient for Flexural Vibrations of Beams," Proc. of the 2nd U. S. National Congress on Applied Mechanics, Published by ASME, 1954.

29. Neal, B. G. "Effect of Shear Force on the Fully Plastic Moment of an I-Beam," Journal of Mechanical Engineering Sciences, Vol. 3, No. 3, September 1961.

30. Neal, B. G. "The Effect of Shear and Normal Forces on the Fully Plastic Moment of an I-Beam of Rectangular Cross-Section," Journal of Applied Mechanics, Vol. 28, No. 2, June 1961.

31. Neal, B. G. "The Plastic Methods of Structural Analysis," Chapman and Hall, London, 1956.

32. Newmark, N. M. "A Method of Computation for Structural Dynamics," Trans. of the ASCE, Vol. 127, 1962.

33. Plass Jr., H. J. "Timoshenko Beam Equation for Short Pulse-Type Loading," Journal of Applied Mechanics, Vol. 25, No. 3, September 1958.

34. Prager, W. "An Introduction to Plasticity," Addison-Wesley Pub. Co., Inc., 1959.

35. Rawlings, B. "Dynamic Behavior of a Rigid-Plastic Steel Beam," The Journal of Mechanical Engineering Science, Vol. 4, No. 1, March 1962.

36. Rayleigh, W. "Theory of Sound," Cambridge, England, 1877.

37. Rodden, W. P., Jones, J. P. and Bhuta, P. G. "A Matrix Formulation of the Transverse Structural Influence Coefficients of an Axially Loaded Timoshenko Beam," AIAA Journal, Vol. 1, No. 1, January 1963, Technical Notes and Comments.

38. Salvadori, M. G. and Weidlinger, P. "On the Dynamic Strength of Rigid-Plastic Beams Under Blast Loads," Journal of the Engineering Mechanics Division, Proc. of the ASCE, Vol. 83, No. EM4, October 1957.

39. Snowden, J. C. "Response of a Simply Clamped Beam to Vibratory Forces and Moments," The Journal of the Acoustical Society of America, Vol. 36, No. 3, March 1964.

40. Szidarovszky, J. "Natural Vibration of a Bar under Axial Force, Taking into Consideration the Effect of Shearing Force and Rotatory Inertia," Acta Tech. Acad. Sci. Hungaricae, Budapest, 39 1/2, 1962.

41. Timoshenko, S. "Vibration Problems in Engineering," D. Van Nostrand Co., N. Y., 1928.

42. Toridis, T. G. "Dynamic Behavior of Elasto-Inelastic Beams Subjected to Moving Loads," Doctoral Dissertation, Civil Engineering Department, Michigan State University, September 1964.

43. Tseitlin, A. I. "On the Effect of Shear Deformation and Rotatory Inertia in Vibrations of Beams on Elastic Foundations," Applied Mathematics and Mathematics, 25, 2, 1961.

44. Tung, T. P. and Newmark, N. M. "A Review of Numerical Integration Methods for Dynamic Response of Structures," Civil Engineering Studies, Structural Research Series, No. 69, University of Illinois, Urbana, Illinois, March 1954.

45. Wen, R. K. and Toridis, T. "Discrete Dynamic Models for Elasto-Inelastic Beams," Proc. of the ASCE, Journal of the Engineering Mechanics Division, Vol. 90, No. EM5, Part 1, October 1964.

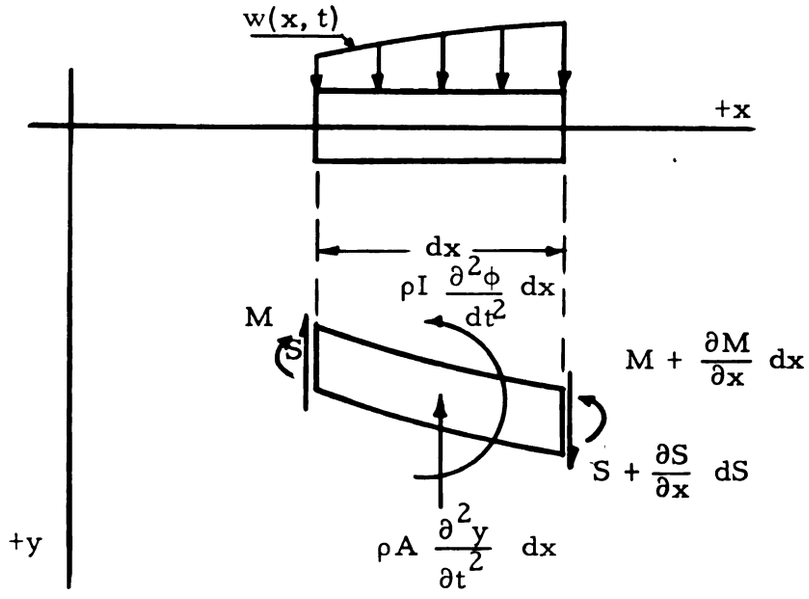

Figure 2.1. Forces Acting on an Element of Continuum.

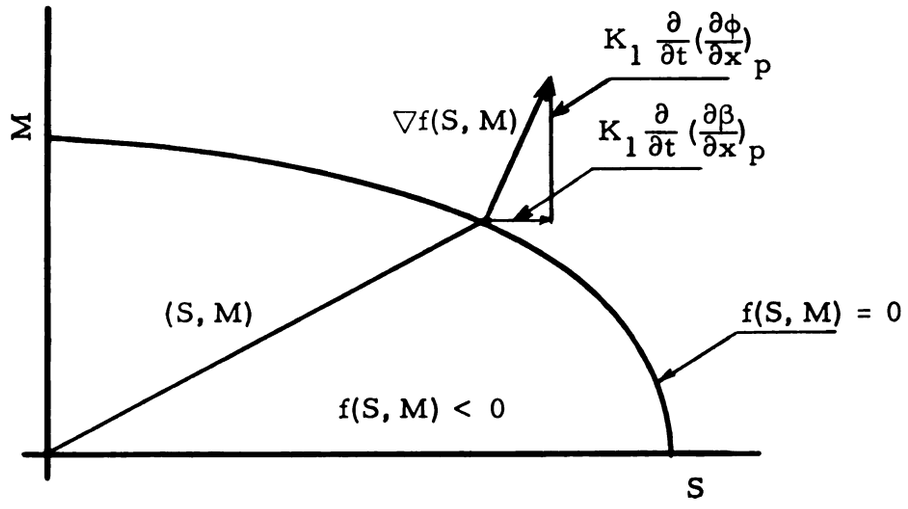

Figure 2.2. Plastic Potential Function.

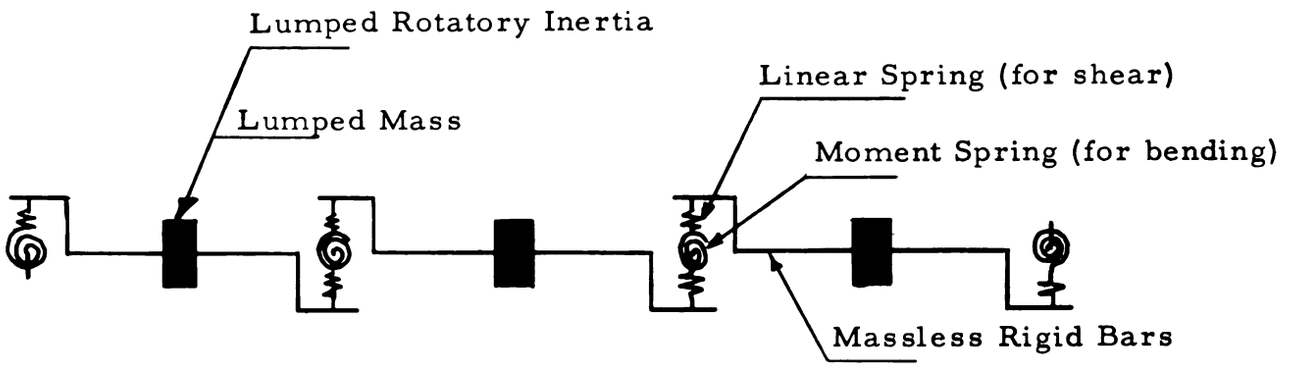

Figure 2.3. Discrete Beam Model

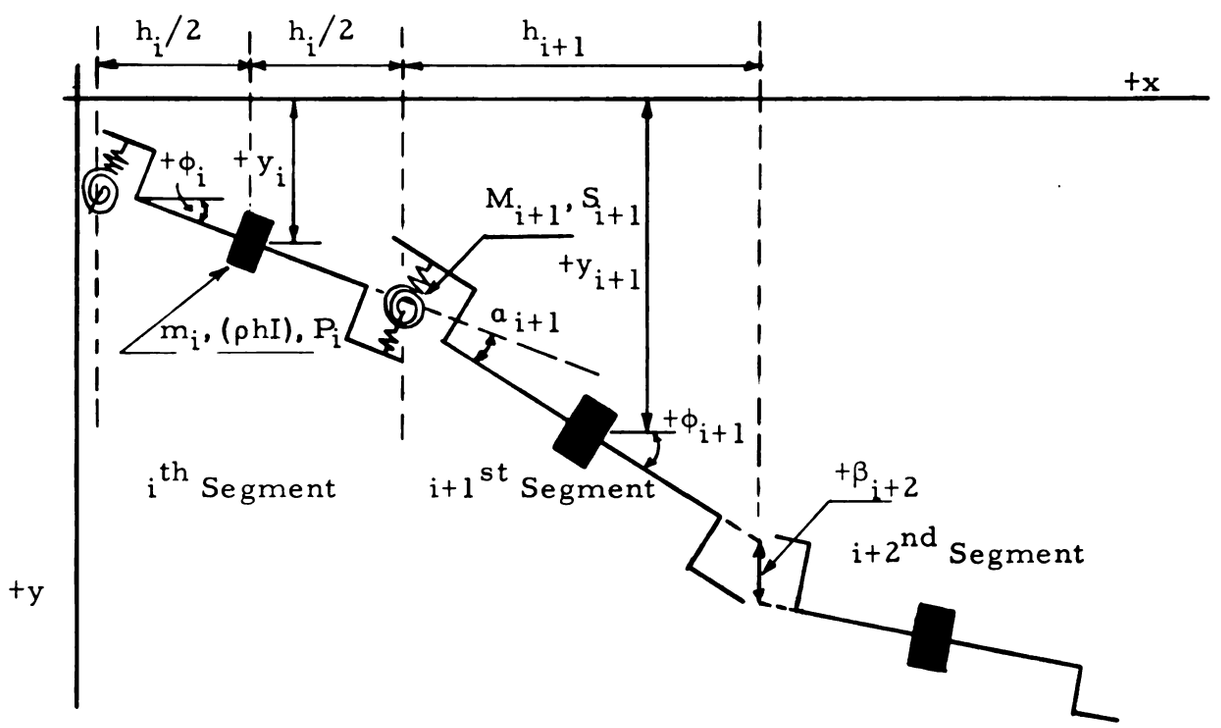

Figure 2.4. Deformed Configuration of the Discrete Beam.

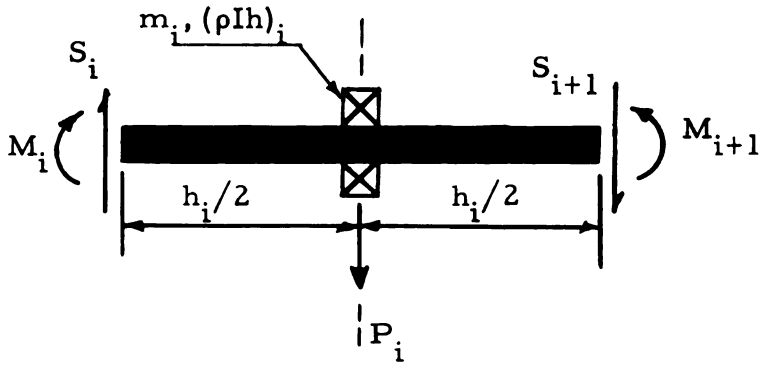

Figure 2.5. Forces Acting on a Typical Panel of the Discrete Beam.

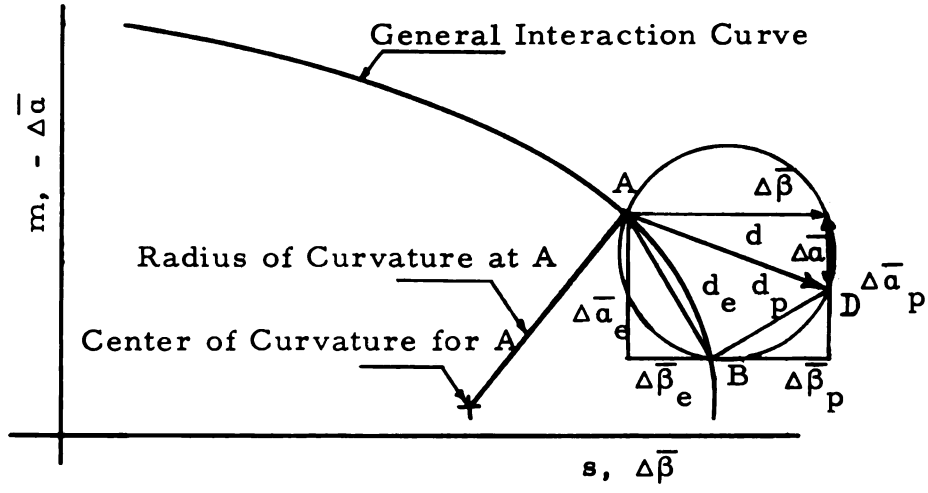

Figure 3.1. Finite Increment Treatment of Plastic Yielding.

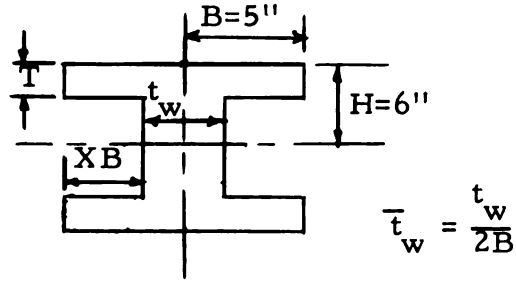

Figure 4.1. Cross-Sectional Properties.

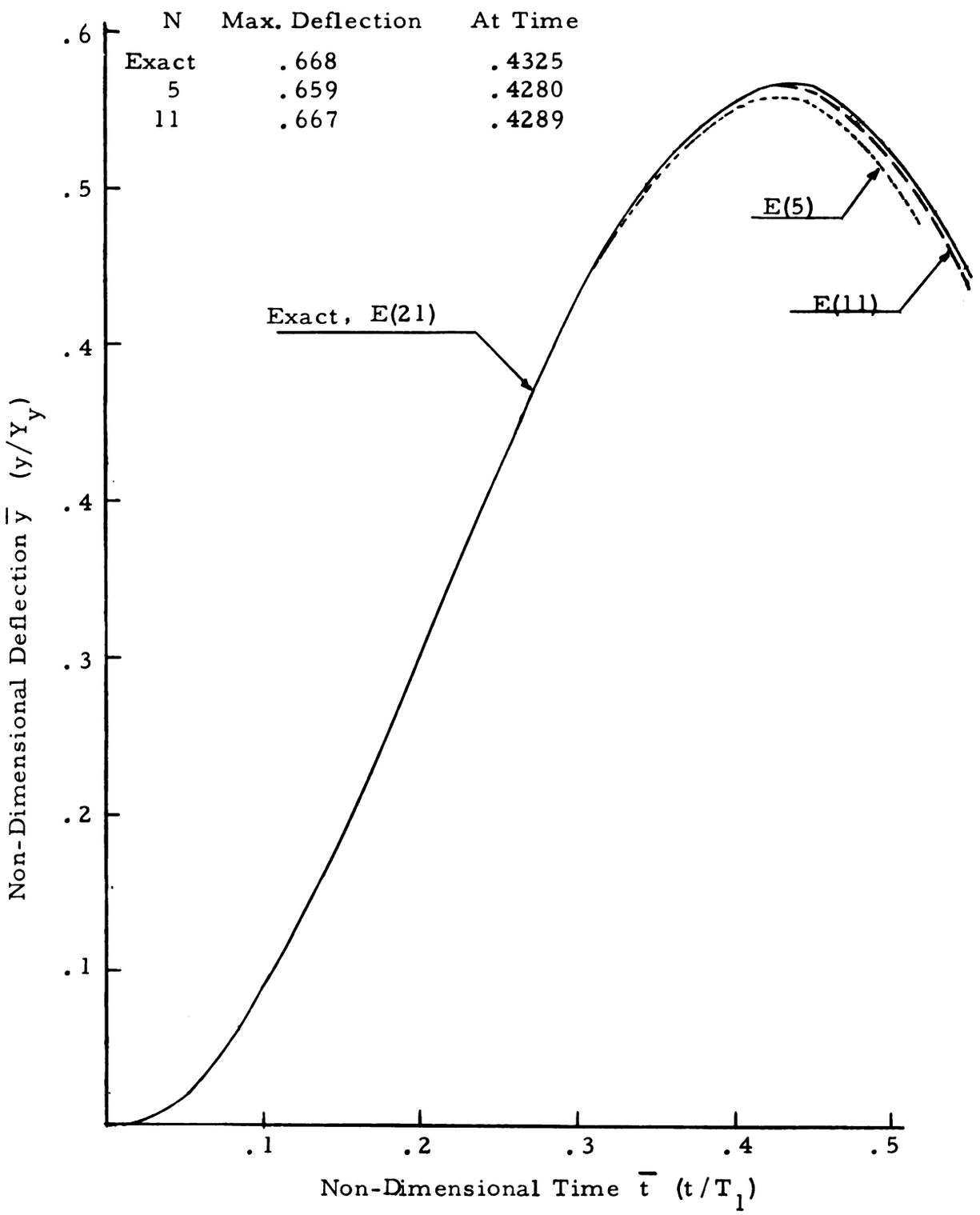

Figure 4.2. Convergence of the "Euler" Model--Deflection at Mid-span.

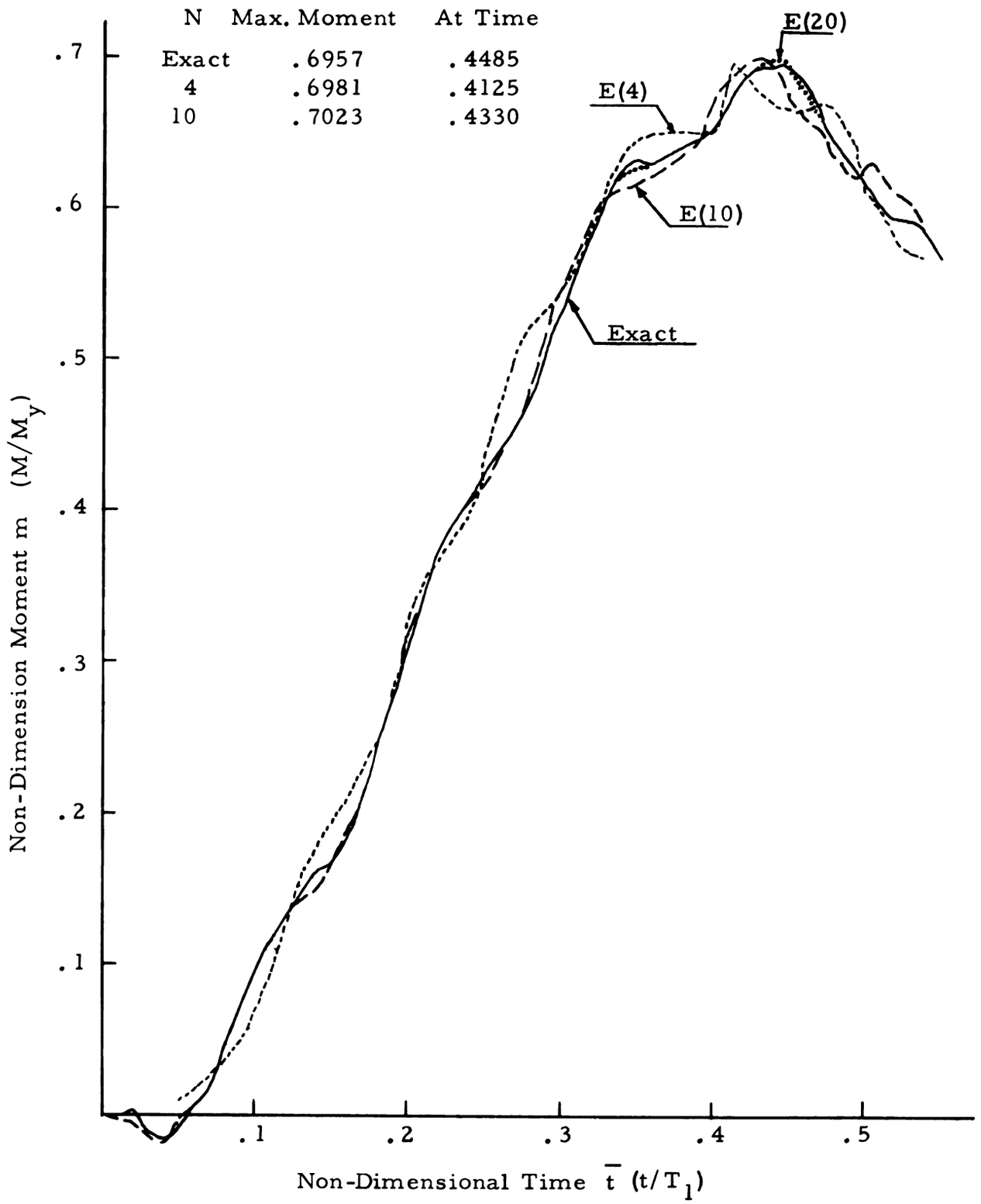

Figure 4.3. Convergence of the "Euler" Model--Moment at Mid-span.

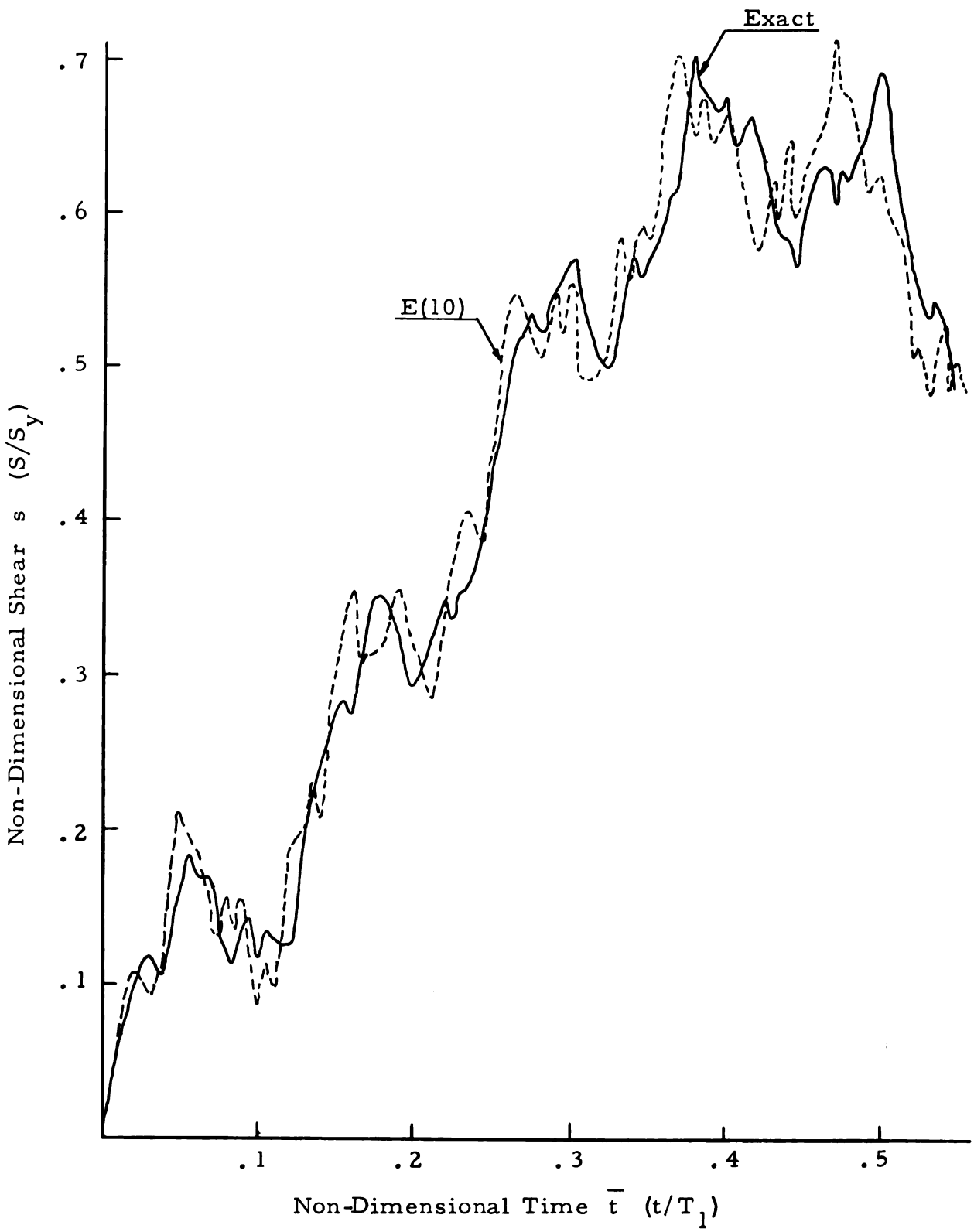

Figure 4.4. Convergence of the "Euler" Model--Shear at the Support.

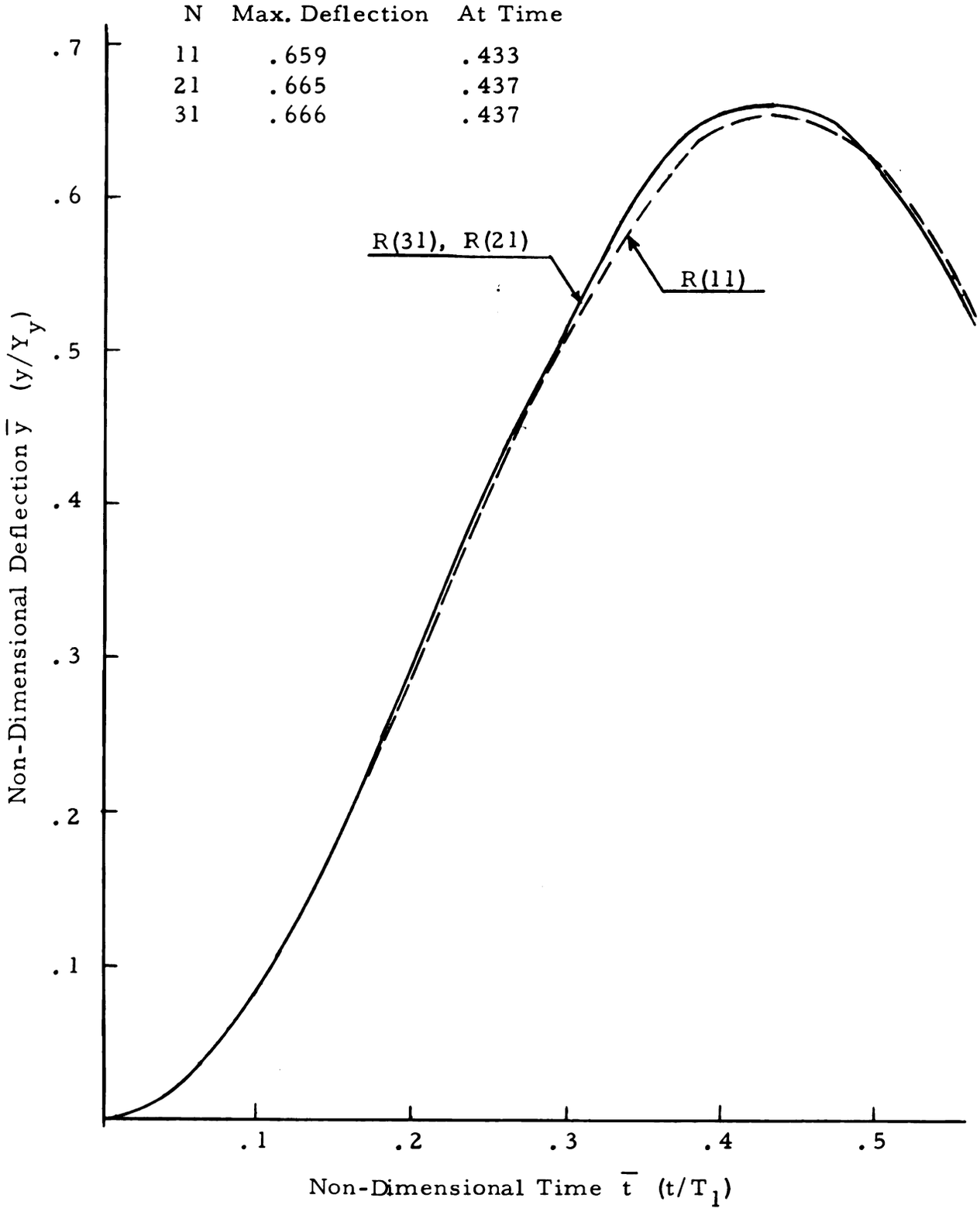

Figure 4.5. "Apparent" Convergence of the "Rotary" Model--Deflection at Mid-span.

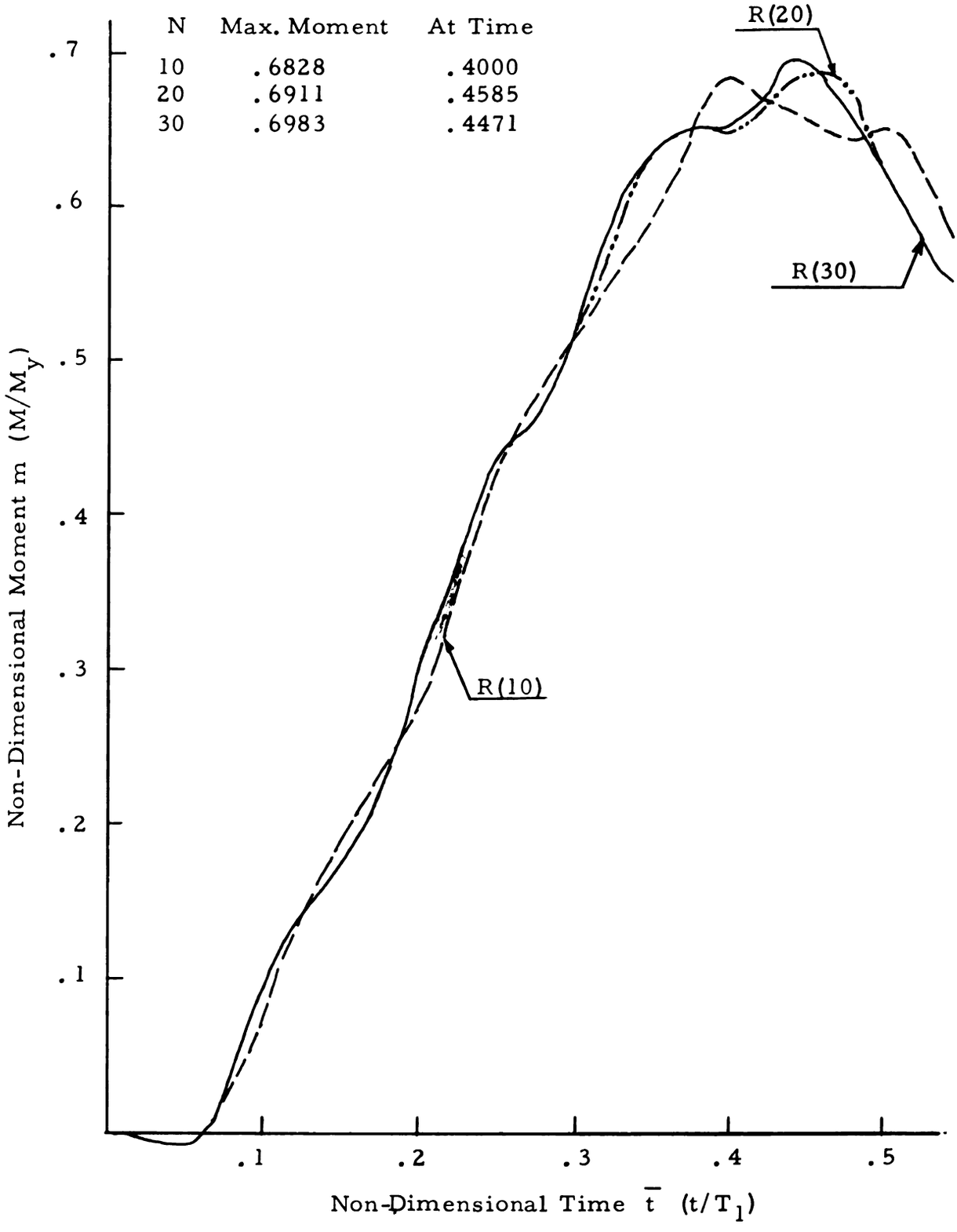

Figure 4.6. "Apparent" Convergence of the "Rotary" Model--Moment at Mid-span.

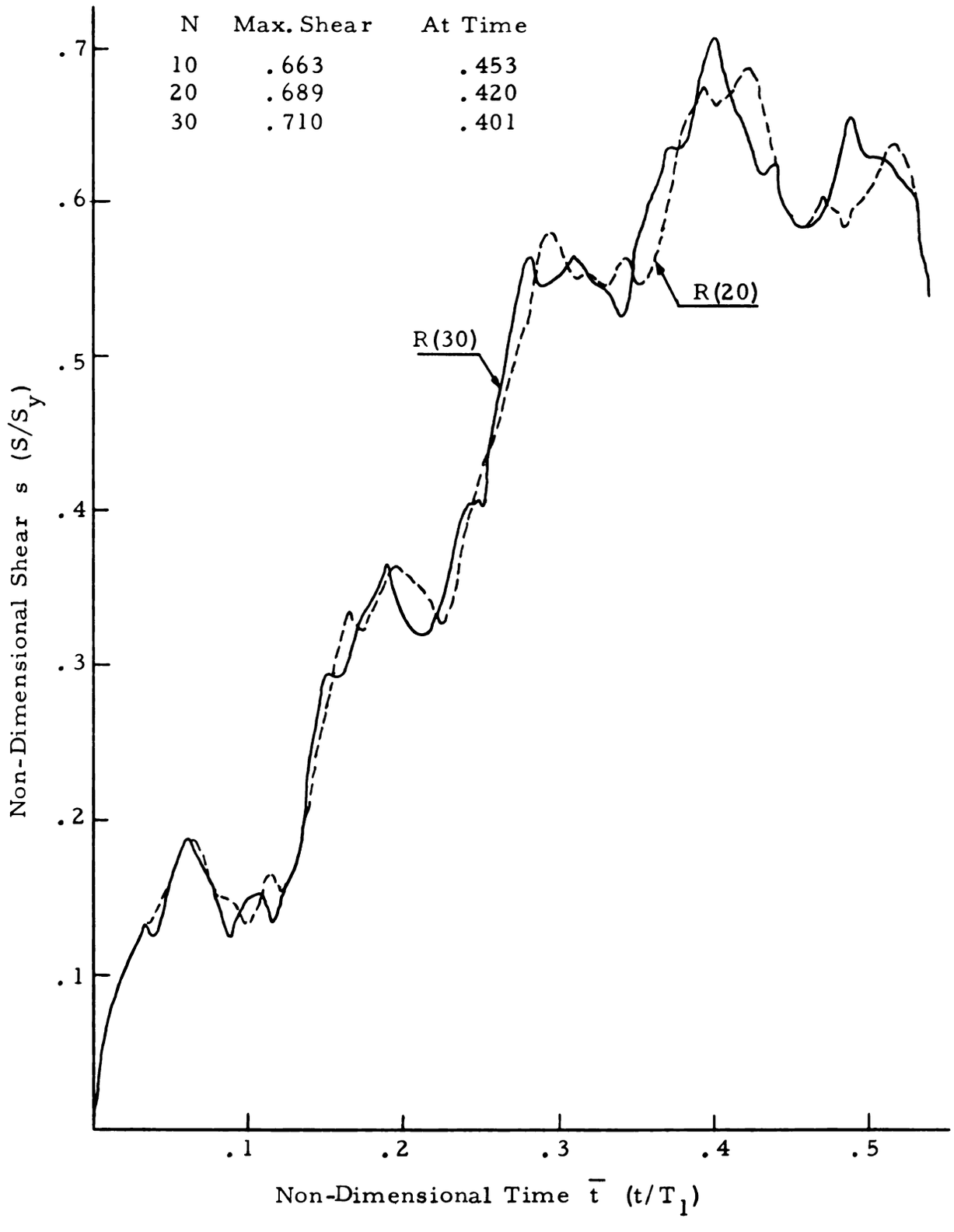

Figure 4.7. "Apparent" Convergence of the "Rotary" Model--Shear at the Support.

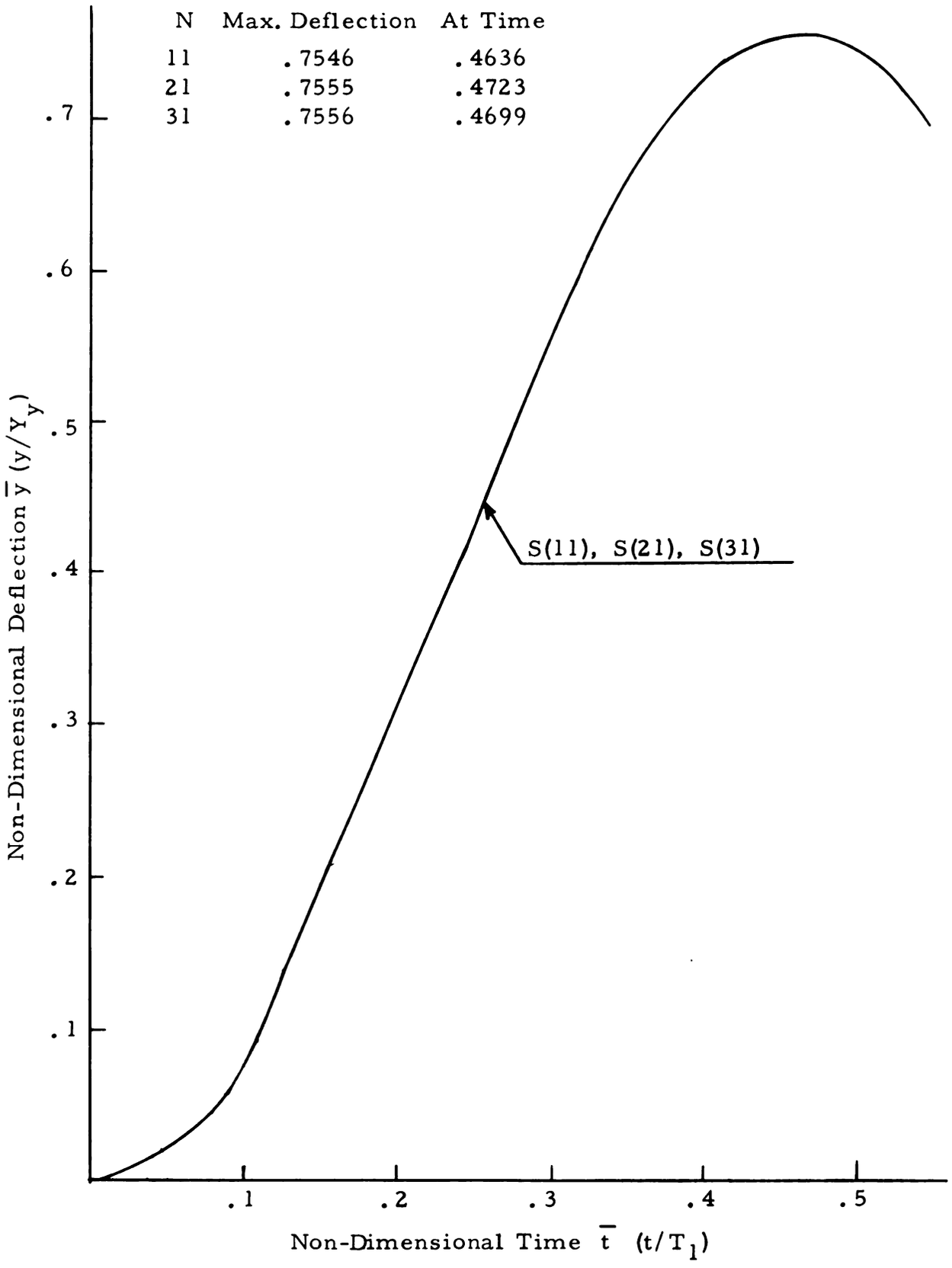

Figure 4.8. "Apparent" Convergence of the "Shear Model--Deflection at Mid-span.

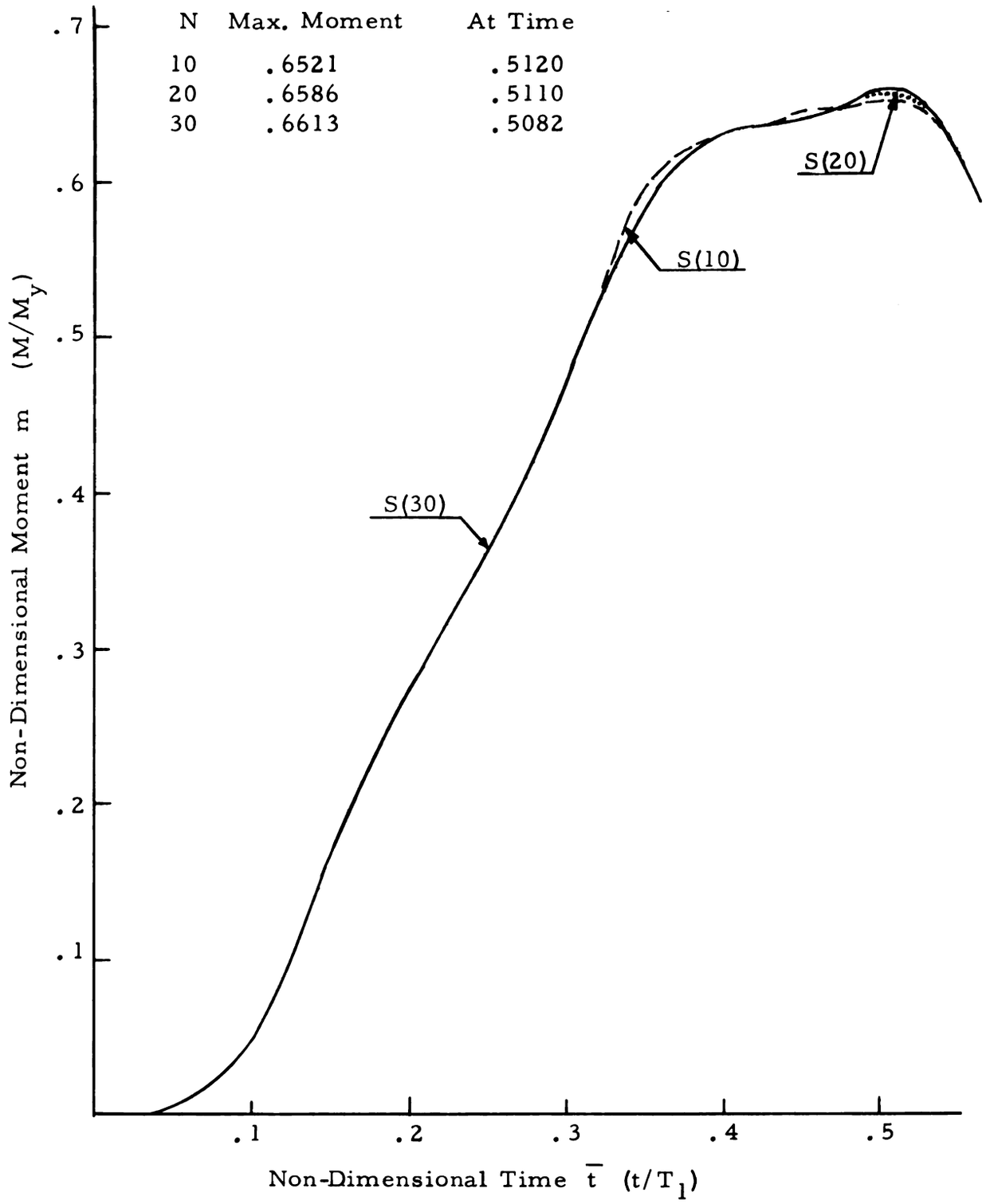

Figure 4.9. "Apparent" Convergence of the "Shear" Model--Moment at Mid-span.

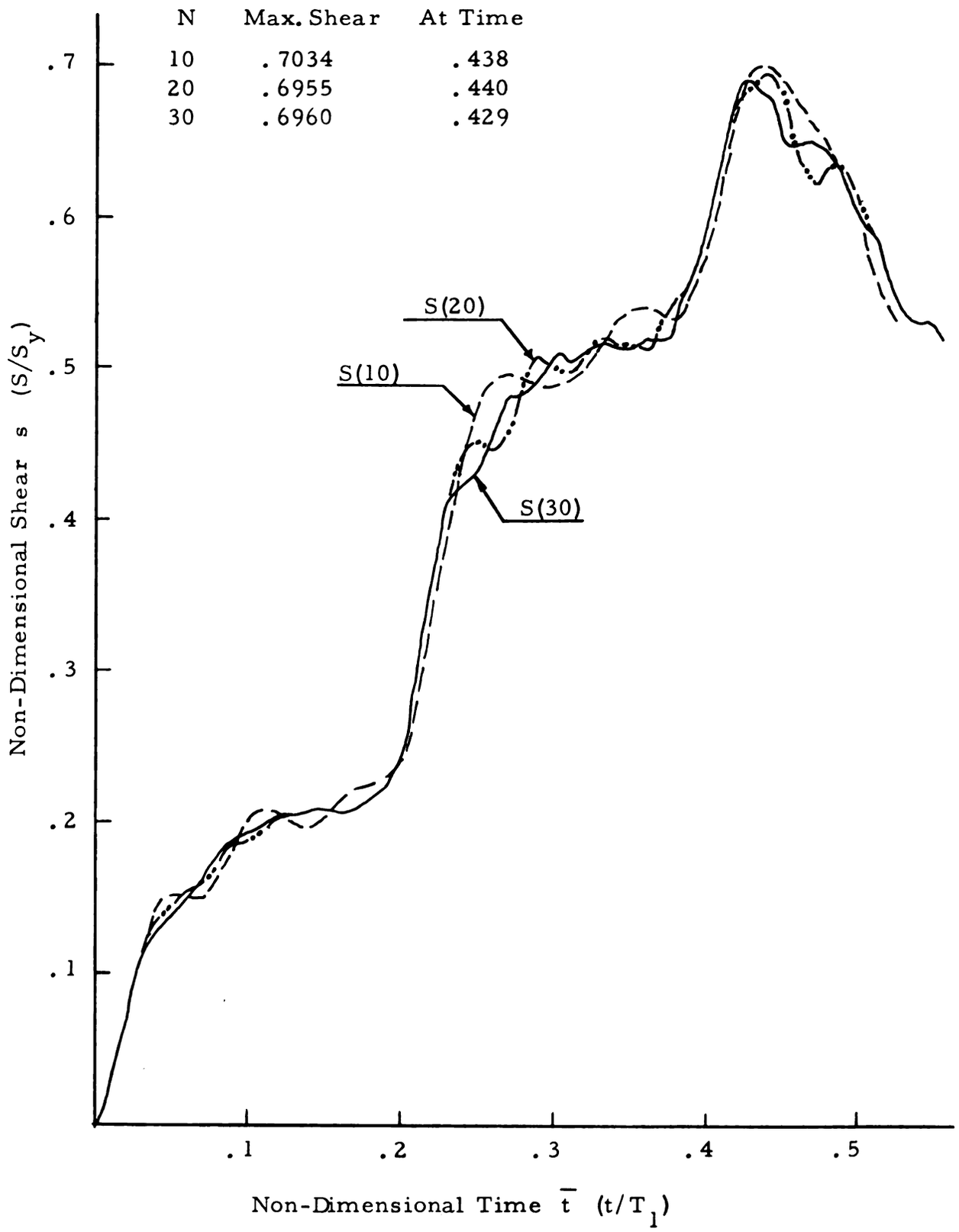

Figure 4.10. "Apparent" Convergence of the "Shear" Model--Shear at the Support.

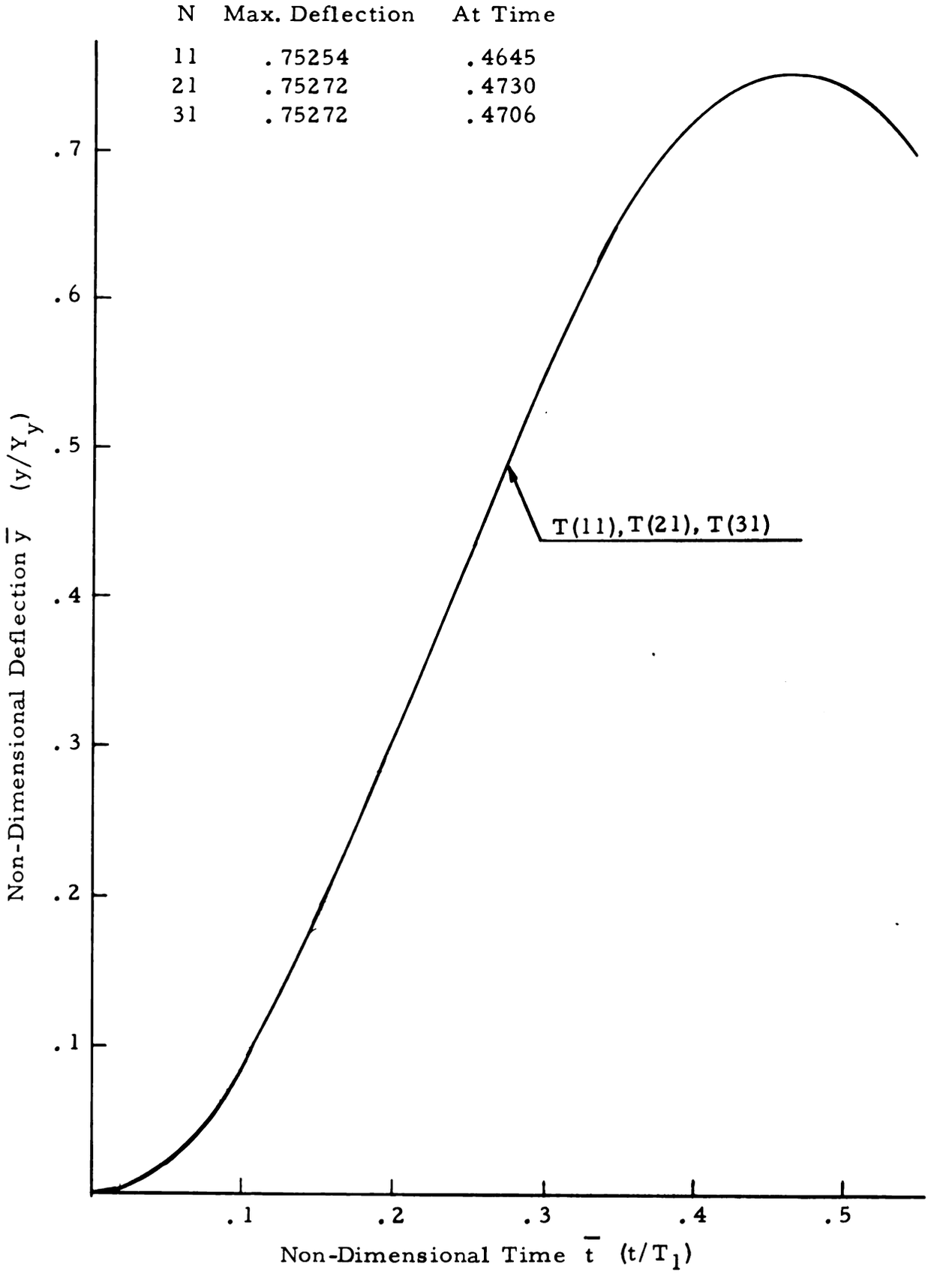

Figure 4.11. "Apparent" Convergence of the "Timoshenko" Model--Deflection at Mid-span.

(M/M_c)

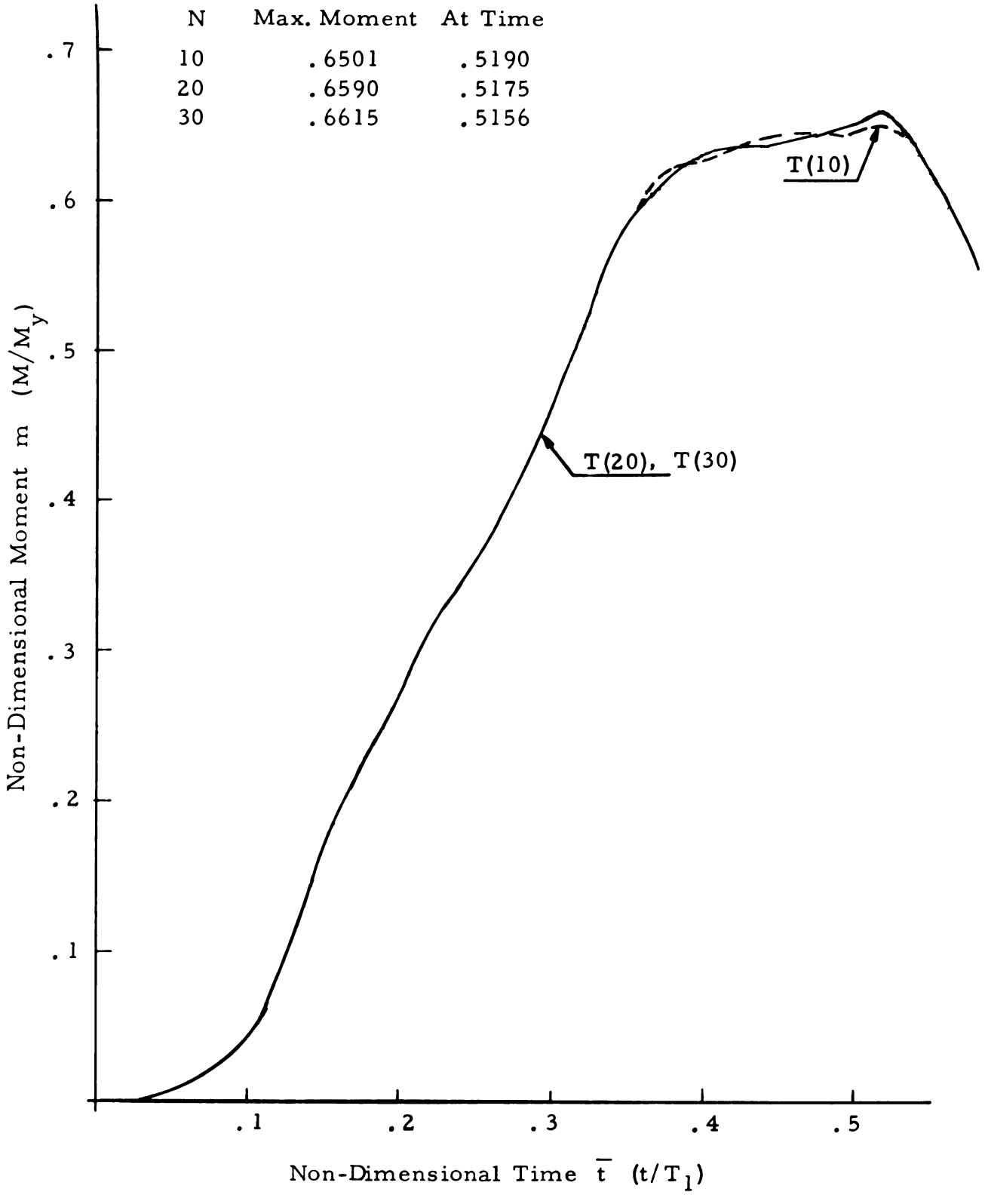

Figure 4.12. "Apparent" Convergence of the "Timoshenko" Model--Moment at Mid-span.

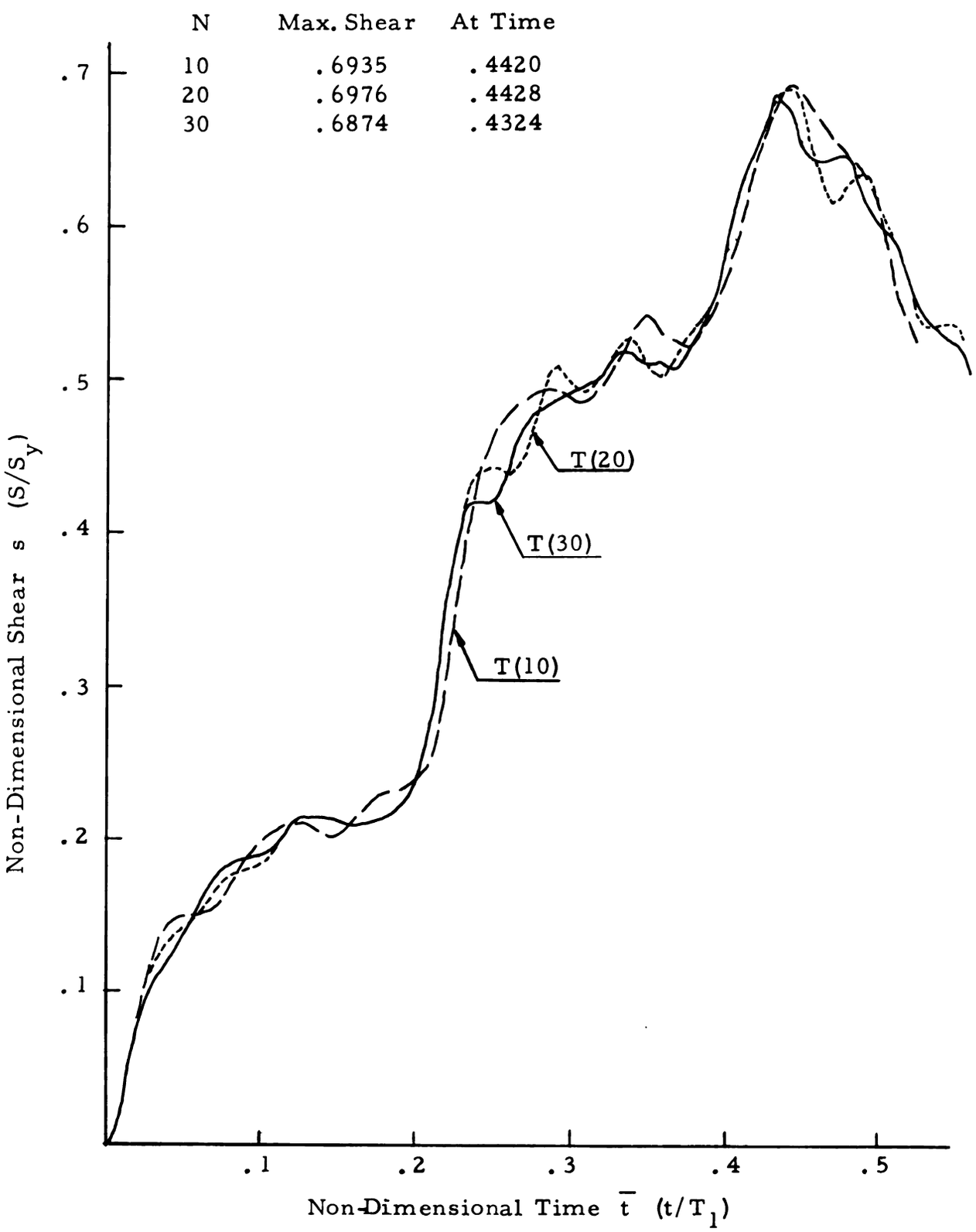

Figure 4.13. "Apparent" Convergence of the "Timoshenko" Model --Shear at the Support.

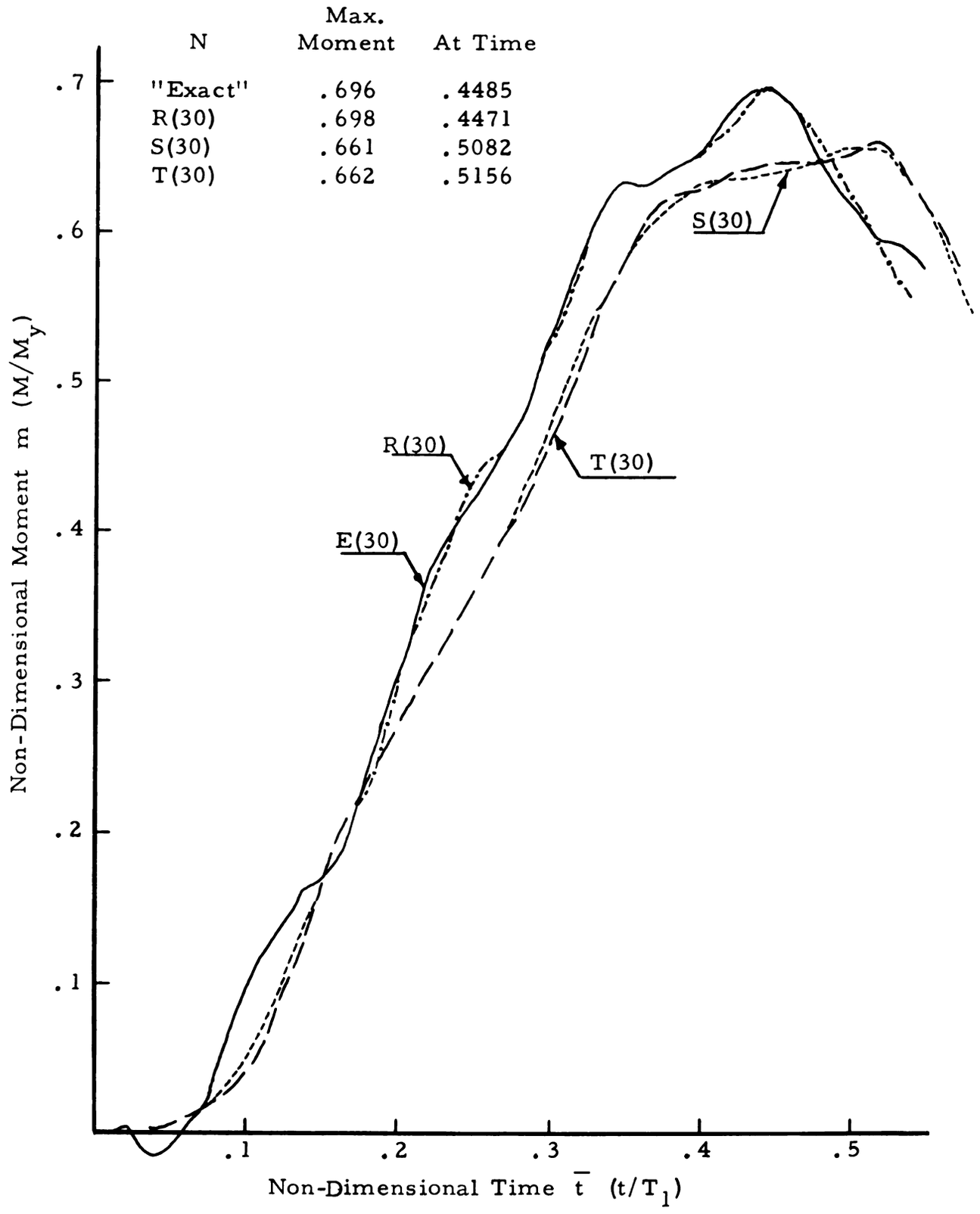

Figure 4.14. Mid-span Moment Responses.

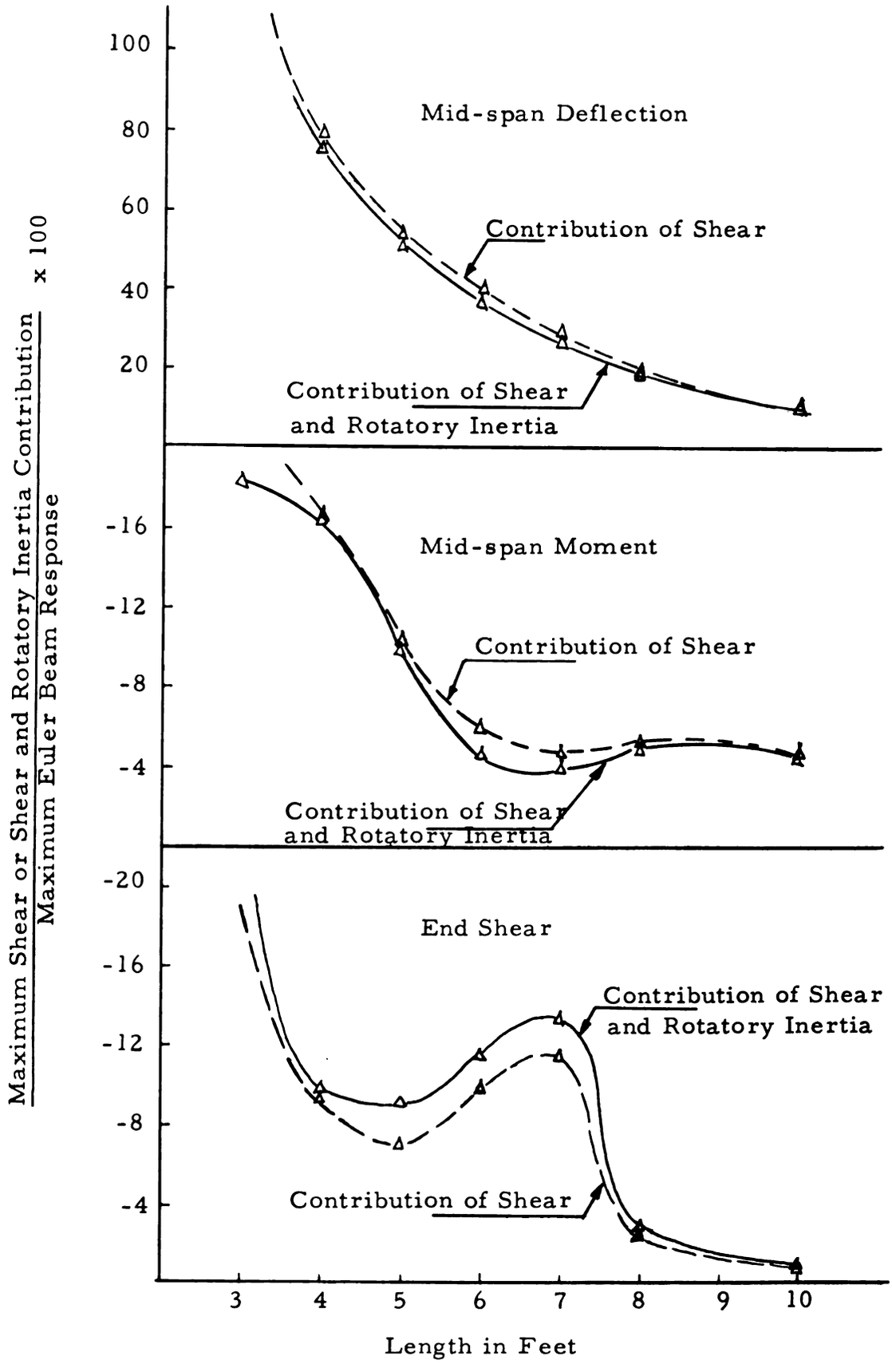

Figure 4.15. Influence of Shear, and Shear and Rotatory Inertia in the Elastic Range.

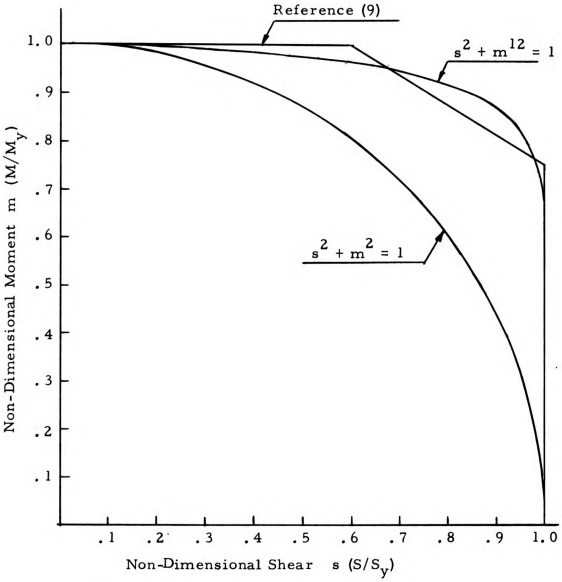

Figure 5.1. Shear-Moment Interaction Curves.

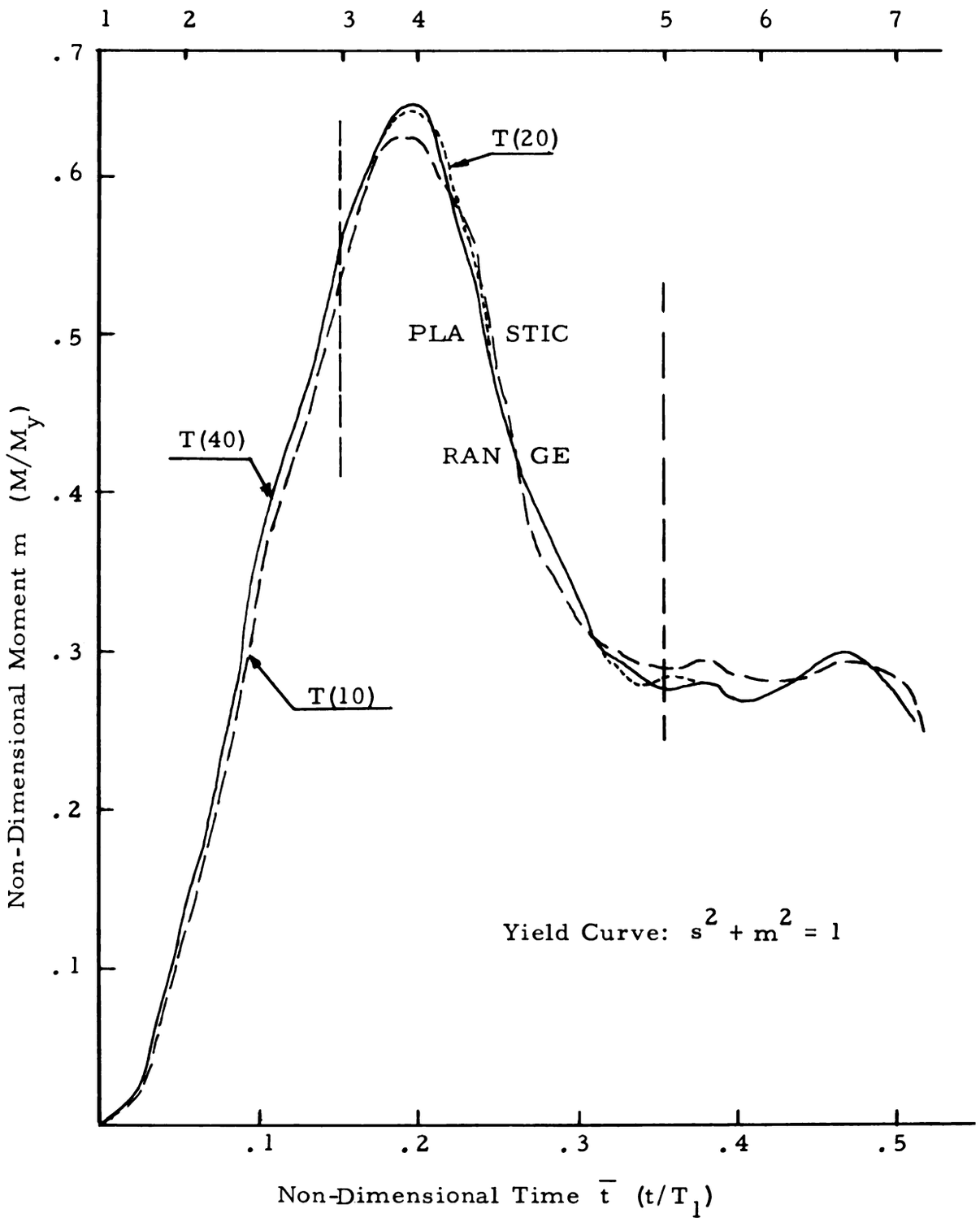

Figure 5.2. "Apparent" Convergence of the "Timoshenko" Model in Elastic-Plastic Response -- Moment at Fixed End.

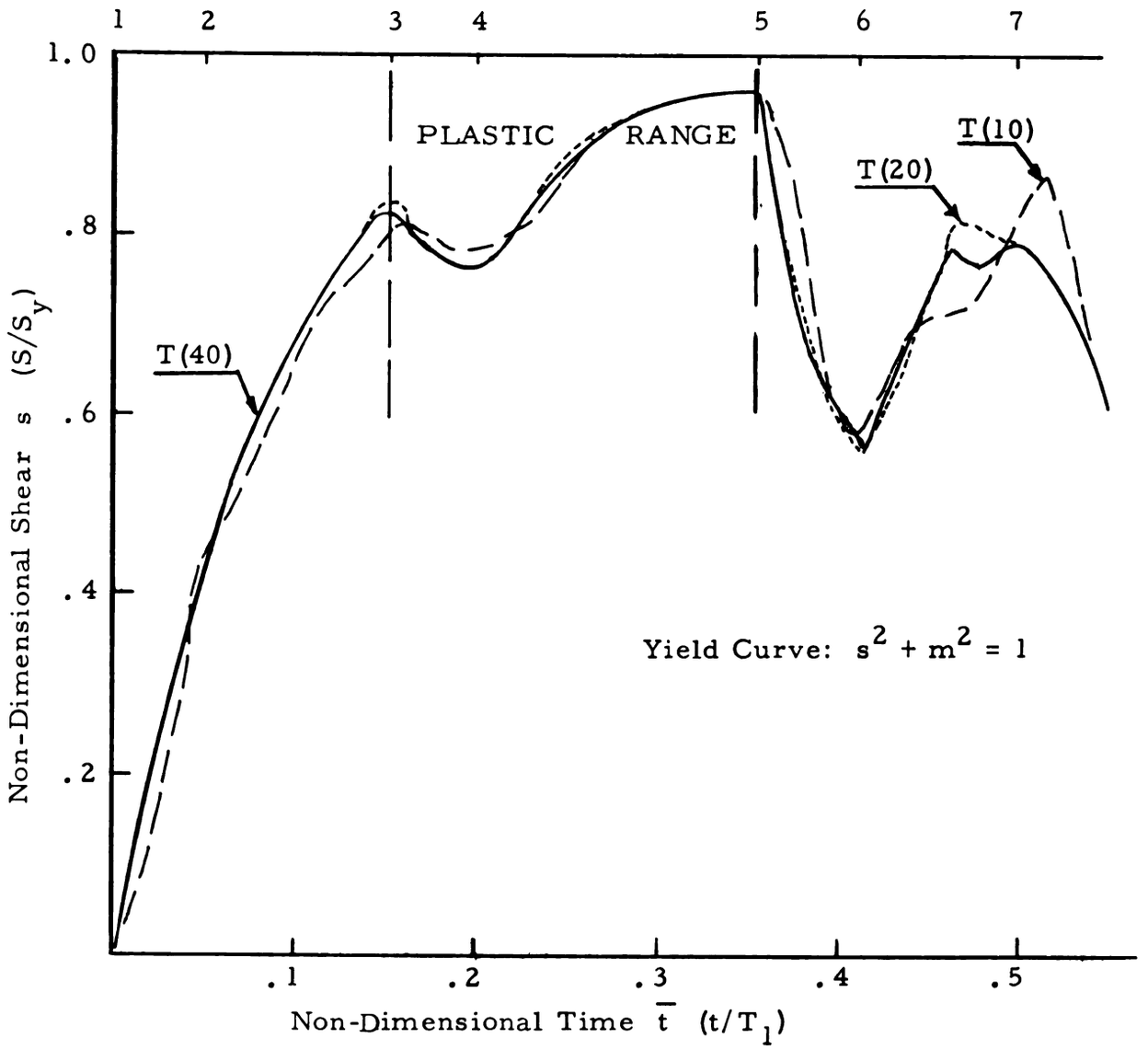

Figure 5.3. "Apparent" Convergence of "Timoshenko" Model in Elastic-Plastic Response -- Shear at Fixed End.

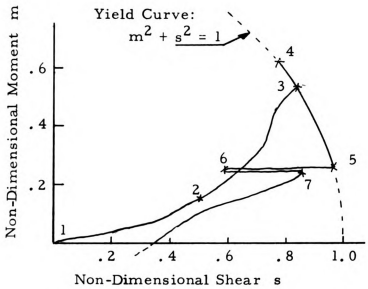

Figure 5.4. Locus of Stress State for Problem in Figures 5.2 and 5.3.

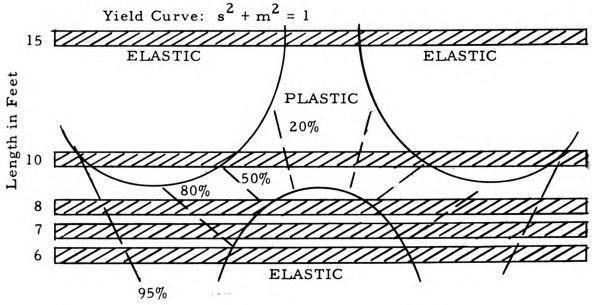

Figure 5.5. Regions of Plastic Response for Simply Supported I-Beams with Different Lengths.

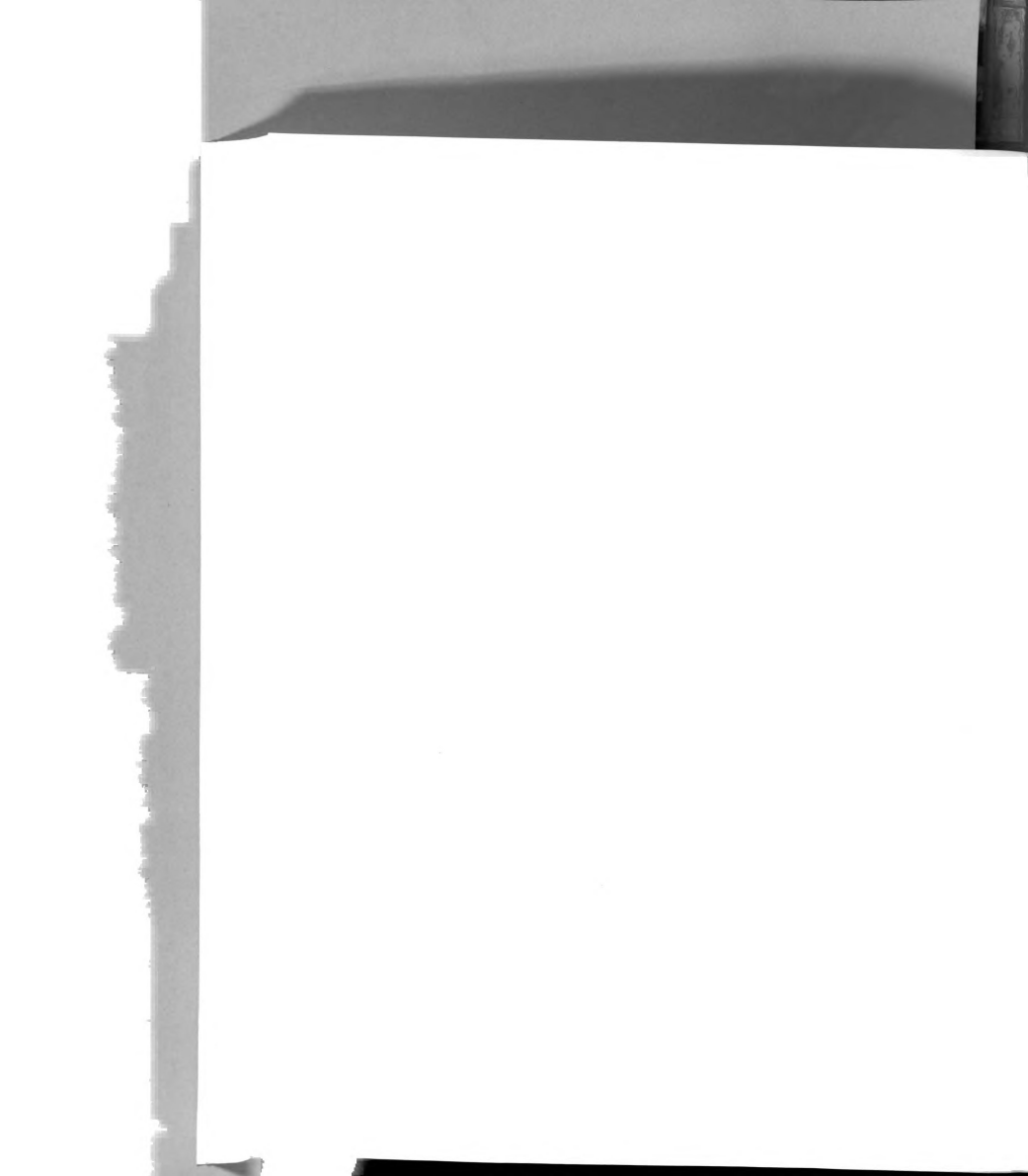

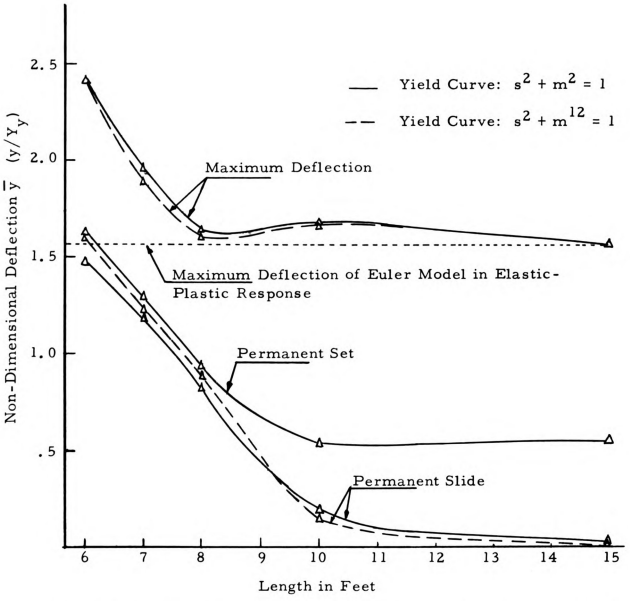

Figure 5.6. Deflections, Permanent Sets, and Permanent Slides for Simply Supported I-Beams with Different Lengths.

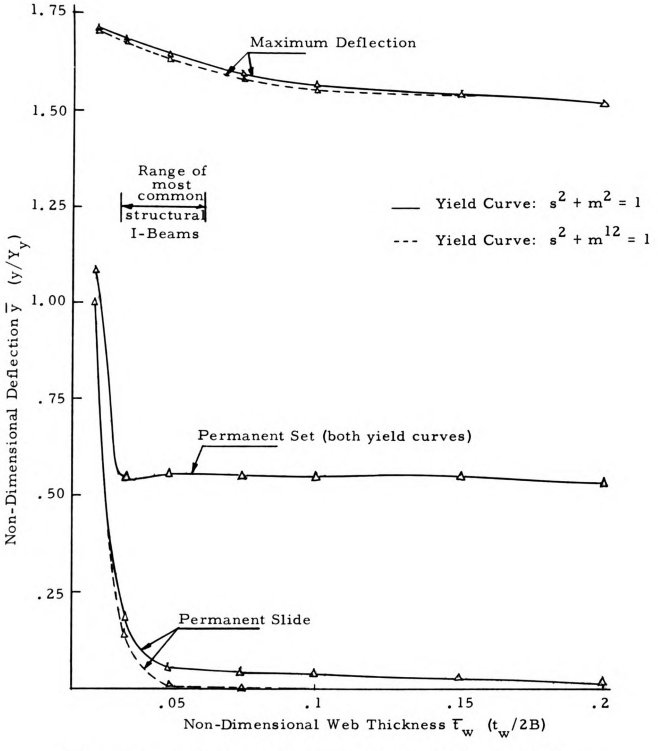

Figure 5.7. Deflections, Permanent Sets, and Permanent Slides for Simply Supported I-Beams with Different Thicknesses.

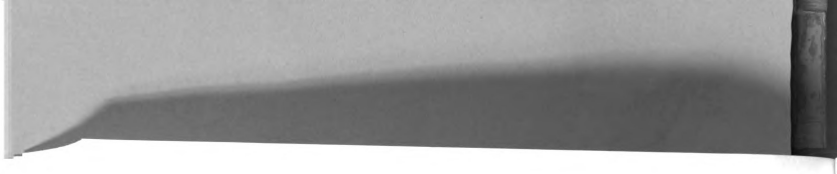

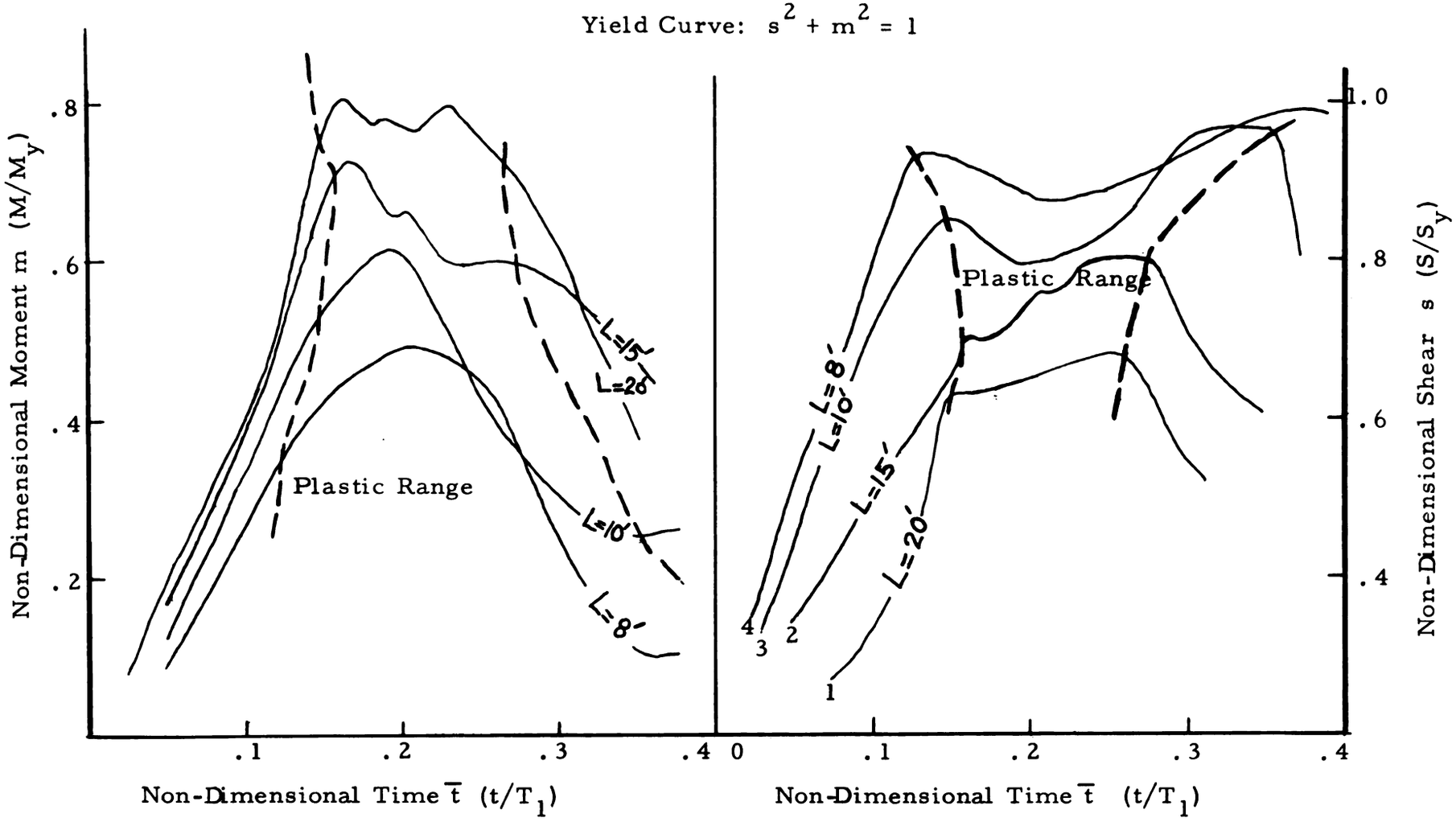

Figure 5.8. Fixed-End Moment and Shear Responses of I-Beams with Different Lengths.

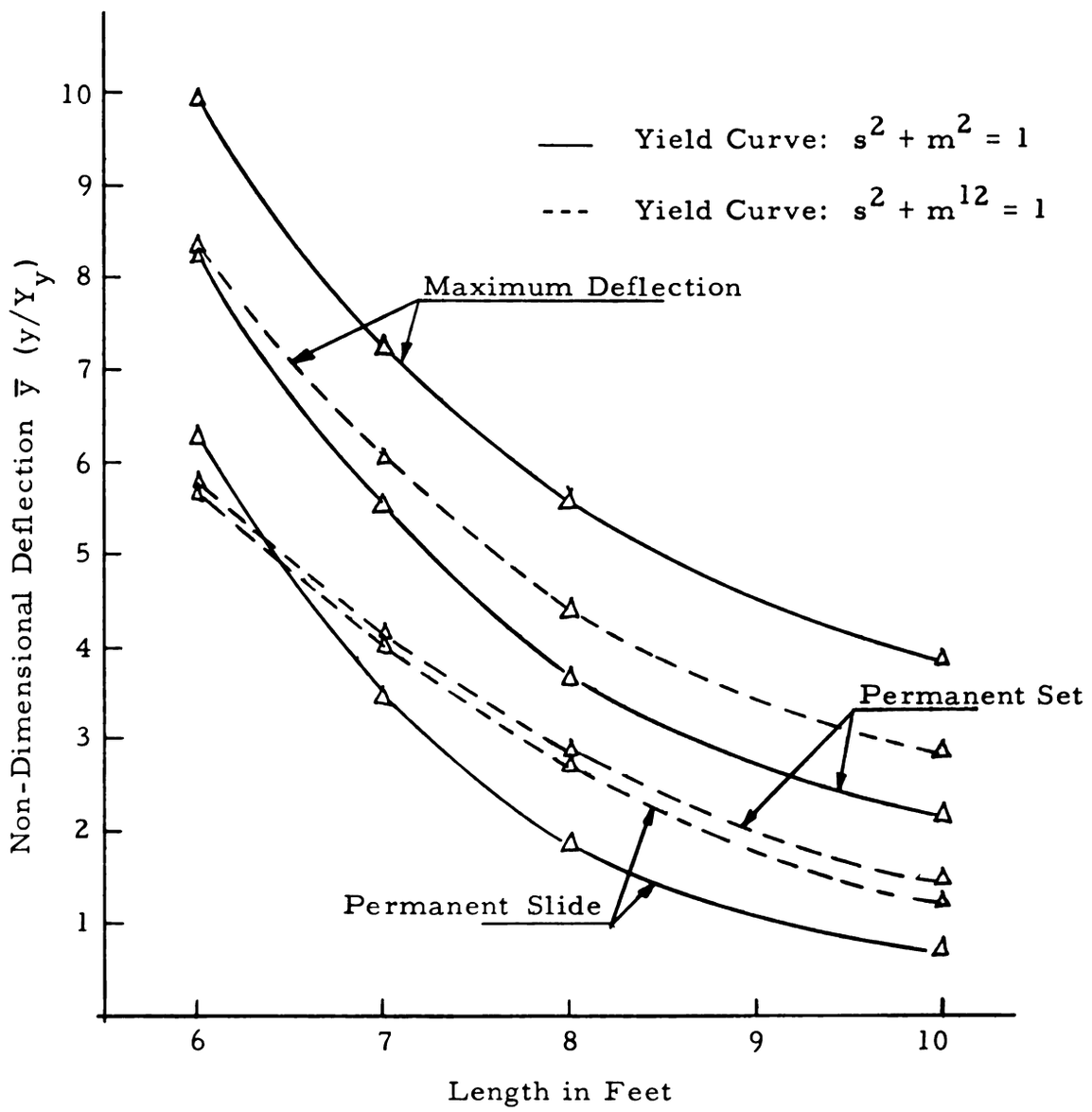

Figure 5.9. Deflections, Permanent Sets, and Permanent Slides for Fixed-Fixed I-Beams with Different Lengths.

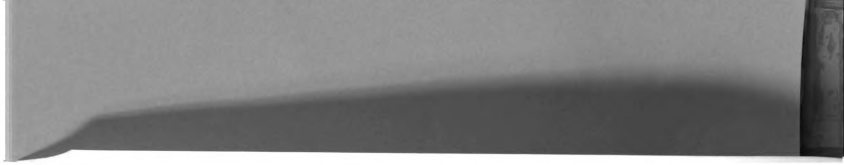

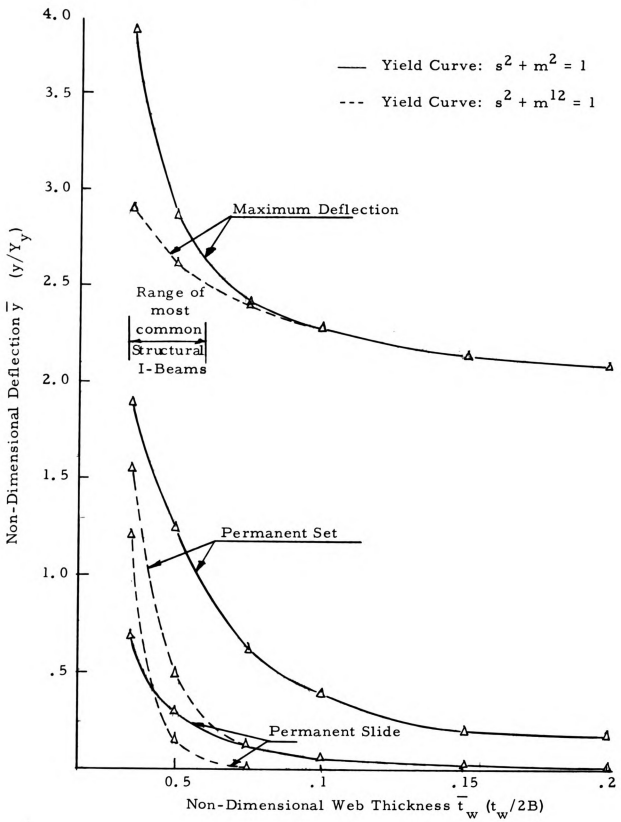

Figure 5.10. Deflections, Permanent Sets, and Permanent Slides for Fixed-Fixed I-Beams with Different Web Thicknesses.

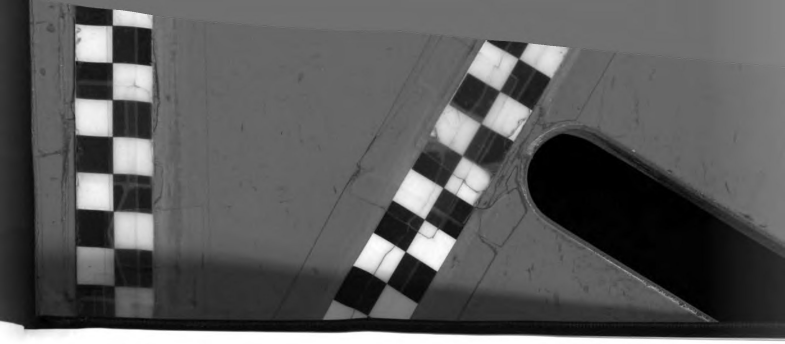

APPENDIX

"EXACT" ELASTIC SOLUTION OF EULER BEAM

For a uniform, simply supported beam subjected to a uniformly applied load $cW\, e^{-2t/T_1}$, the deflection is readily found to be

$$y(x,t) = \sum_{i=1,3,\ldots,}^{\infty} \frac{4Wc}{\pi\rho A} \sin\frac{i\pi x}{L} \left(\frac{p_i e^{-2t/T_1} - p_i \cos(p_i t) + \frac{2}{T_1}\sin(p_i t)}{i p_i \left(p_i^2 + \frac{4}{T_1^2}\right)} \right)$$

The bending moment M, and the shear S can be computed, respectively, from the second and third derivatives of the deflection function.

If the loading W is written in terms of the yield moment ($W = 8\, M_y/L^2$), the responses can be made non-dimensional as follows,

$$\bar{y}(\zeta,\bar{t}) = \sum_{i=1,3}^{\infty} \frac{1536 \sin i\pi\bar{t}}{5i\pi^3(\pi^2 i^4+1)} \left(e^{-2\bar{t}} - \cos 2\pi i^2\bar{t} + \frac{\sin 2\pi i^2\bar{t}}{\pi i^2}\right)$$

$$m(\zeta,\bar{t}) = \sum_{i=1,3}^{\infty} \frac{5i^2\pi^3 c}{48}\, y(\zeta,\bar{t})$$

$$s(\zeta,\bar{t}) = \sum_{i=1,3}^{\infty} \frac{5i^3\pi^3 c}{48}\frac{M_y}{S_y L}\, y(\zeta,\bar{t})$$

where $\bar{t} = t/T_1$, $\zeta = x/L$.

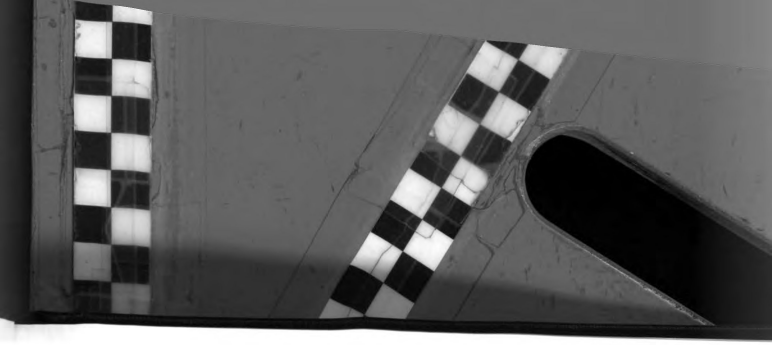

It is of interest that through this non-dimensionalization process, no material and physical properties appear in the expressions for deflection and moment. (Indeed, the choice of $W = 8\ M_y / L^2$ made this possible in the case of the moment.)

It may be noted that all of these expressions are convergent. The deflection converges at $1/i^5$, the moment converges as $1/i^3$, and shear converges as $1/i^2$.